NeuroImage 245 (2021) 118630

Contents lists available at ScienceDirect

NeuroImage

journal homepage: www.elsevier.com/locate/neuroimage

Contribution of animal models toward understanding resting state functional connectivity

Patricia Pais-Roldán[a], Celine Mateo[b], Wen-Ju Pan[c], Ben Acland[d], David Kleinfeld[b,e], Lawrence H. Snyder[d], Xin Yu[f], Shella Keilholz[c,*]

[a] Medical Imaging Physics, Institute of Neuroscience and Medicine 4, Forschungszentrum Jülich 52425, Germany
[b] Department of Physics, University of California San Diego, La Jolla, CA 92093, USA
[c] Wallace H. Coulter Department of Biomedical Engineering, Emory University/Georgia Institute of Technology, Atlanta, GA 30322, USA
[d] Department of Neuroscience, Washington University School of Medicine, Saint Louis, MO 63110, USA
[e] Section of Neurobiology, University of California, La Jolla, San Diego, CA 92093, USA
[f] Athinoula A. Martinos Center for Biomedical Imaging, Massachusetts General Hospital and Harvard Medical School, Charlestown, MA 02129, USA

A B S T R A C T

Functional connectivity, which reflects the spatial and temporal organization of intrinsic activity throughout the brain, is one of the most studied measures in human neuroimaging research. The noninvasive acquisition of resting state functional magnetic resonance imaging (rs-fMRI) allows the characterization of features designated as functional networks, functional connectivity gradients, and time-varying activity patterns that provide insight into the intrinsic functional organization of the brain and potential alterations related to brain dysfunction. Functional connectivity, hence, captures dimensions of the brain's activity that have enormous potential for both clinical and preclinical research. However, the mechanisms underlying functional connectivity have yet to be fully characterized, hindering interpretation of rs-fMRI studies. As in other branches of neuroscience, the identification of the neurophysiological processes that contribute to functional connectivity largely depends on research conducted on laboratory animals, which provide a platform where specific, multi-dimensional investigations that involve invasive measurements can be carried out. These highly controlled experiments facilitate the interpretation of the temporal correlations observed across the brain. Indeed, information obtained from animal experimentation to date is the basis for our current understanding of the underlying basis for functional brain connectivity. This review presents a compendium of some of the most critical advances in the field based on the efforts made by the animal neuroimaging community.

1. Introduction

Functional magnetic resonance imaging (fMRI) and its sibling resting state fMRI (rs-fMRI) are currently our most powerful tools for noninvasive functional imaging of the whole brain. Together, they have provided insight into systems-level features related to cognition and behavior, and how those features are altered in neurological and psychiatric disorders. Compared to task-based fMRI (Bandettini et al., 1992; Menon et al., 1992), where the timing of the task or stimulus is known and can be used to identify the brain areas that are activated, rs-fMRI is more difficult to interpret. The blood oxygenation level-dependent (BOLD (Ogawa et al., 1990)) fluctuations that are produced in response to the brain's intrinsic activity exhibit spatial and temporal structure that have been summarized into functional connectivity matrices (Allen et al., 2014), functional networks (Yeo et al., 2011), and functional connectivity gradients (Margulies et al., 2016), to name a few of the most common interpretations. While rs-fMRI has become immensely popular due to its ability to characterize activity noninvasively throughout the whole brain, the simplicity of the acquisition paradigm, and the lack of reliance on subject cooperation during task performance, it remains poorly understood in the sense that the BOLD fluctuations arise from a combination of neurophysiological processes, and alterations in any single component can affect the downstream calculation of functional connectivity-based features.

BOLD is an integrative signal that reflects a combination of hemodynamic effects (Buxton et al., 1998; Friston et al., 2000), including total vascular volume and metabolically-driven changes in the ratio of oxygenated to deoxygenated hemoglobin (Silva et al., 1999; Kida et al., 2000), which occur in response to neural activity (Brinker et al., 1999; Logothetis et al., 2001). Differences in functional connectivity observed in separate groups of subjects (healthy vs. patient; fast responder vs. slow responder) could therefore arise from multiple mechanisms (altered anatomical connectivity, altered neural activity, altered vascular properties). Our primary hope of disentangling the BOLD signal lies with multimodal experiments in animal models, where other, often invasive, measurements of particular types of activity can be combined with rs-fMRI. Here we review progress towards a better understanding of the neurophysiology underlying the spontaneous BOLD fluctuations in animal models, with an emphasis on rodents, and highlight areas that are ripe for further exploration.

The simplest approach to understanding how neurophysiological processes give rise to the BOLD fluctuations is to look at localized re-

* Corresponding author.
E-mail address: shella.keilholz@bme.gatech.edu (S. Keilholz).

https://doi.org/10.1016/j.neuroimage.2021.118630.
Received 1 April 2021; Received in revised form 6 August 2021; Accepted 29 September 2021
Available online 10 October 2021.

lationships between neural activity and the resulting hemodynamics. Most of the early studies that provided the first definitive links between neural activity and the BOLD response after presentation of a stimulus took this approach (Brinker et al., 1999; Logothetis et al., 2001), and it has value for understanding the spontaneous BOLD fluctuations as well (Shmuel and Leopold 2008). While it is often assumed that neurovascular coupling is identical whether the activity is intrinsic or task-driven, some studies suggest that the hemodynamic response functions can differ across the two situations (Chen and Glover 2015).

The limitation of focusing on localized relationships between neural activity and the BOLD signal is that the localized approach cannot explain the structured relationships between the BOLD fluctuations from different portions of the brain. Even if we adopt the simplified perspective that correlated BOLD fluctuations reflect correlated neural activity, there are still open issues as to why the neural activity in those brain areas is correlated in the first place. Differences between the structural networks and functional networks derived from the BOLD signal, along with correlations between areas that are known to be weakly connected, are evidence that the simple explanation that correlation reflects communication via a direct white matter connection is inadequate. Going beyond single-site experiments has the potential to reveal not just the neurophysiology of the BOLD signal, but answers to deeper neuroscience questions about the intrinsic functional architecture of the brain.

In this review, we cover mechanisms of localized neurovascular coupling along with investigations that are shedding light into the spatial organization of activity across the brain. For the sake of simplicity, we will often refer to this coordinated activity across different brain areas as functional connectivity, shorthand for the statistical dependencies that are captured by Pearson correlation, independent component analysis (ICA), or other analysis methods.

1.1. Overview of complementary experimental approaches

Functional neuroimaging in healthy human subjects is confined to noninvasive methods such as electroencephalography (EEG), magnetoencephalography (MEG), fMRI, or positron emission tomography (PET), all of which suffer from a combination of limited spatial resolution, limited temporal resolution, lack of whole brain coverage, and lack of specificity. Luckily, both the hemodynamic response to neural activity and the functional networks measured with rs-fMRI are remarkably similar across species (Fox et al., 2005; Vincent et al., 2007; Mantini et al., 2011; Lu et al., 2012; Belcher et al., 2013; Barks et al., 2015; Hsu et al., 2016; Schroeder et al., 2016), making it possible to probe the neurophysiological underpinnings of the BOLD response in animals with a reasonable expectation that the BOLD signal will arise from comparable processes in humans. In animals, tools such as microelectrode arrays, high-resolution optical imaging, and genetic manipulations provide insight into the brain's functional architecture that cannot be obtained in human subjects (Fig. 1).

1.2. Optical imaging

One of the most powerful tools for these investigations is optical imaging, which has the unique capability to capture both intrinsic signals primarily linked to hemodynamics and extrinsic fluorescent signals that directly indicate neuronal activity. Optical extrinsic signals (OES) arise from fluorescence introduced using dyes or genetically-encoded indicators. The development of genetically encoded sensors for the last 20 years has had a profound effect on neuronal circuit dissection. These sensors provide the ability to monitor intracellular calcium, transmembrane voltage, neurotransmitters and a variety of chemicals (Palmer et al., 2011; Oh et al., 2019; Pal and Tian 2020), and can be introduced in cells with virus injections. Also, thanks to the growing availability of Cre-expressing and reporter mice, sensor expression can be targeted specifically to neuronal subtypes, astrocytes, smooth muscle cells, endothelial cells and pericytes in rodents (Hill et al., 2015; Daigle et al., 2018; Tong et al., 2021), to provide an unprecedented level of specificity about the role of different components in the generation of the hemodynamic fluctuations detected with rs-fMRI .

Optical measurements are typically limited to the surface of the brain, but with the growing use of wide-field optical imaging, the field of view has become large enough to capture some of the same spatial structure observed with rs-fMRI in superficial brain regions. Wide-field mesoscale calcium imaging allows the imaging of the cerebral cortex and gives insights into the functional parcellation of the cortex in rodents (Vanni et al., 2017) with a resolution of tens of microns.

Optical intrinsic signals (OIS) can also be mapped using wide-field imaging and have provided critical information about the structure of the vasculature and how it responds to a localized increase in neural activity (Grinvald et al., 1986; Malonek and Grinvald 1996; Hillman 2007). In OIS, no extrinsic contrast agent is required. The most widely-used implementations of OIS imaging are sensitive to changes in light absorption by oxy- and deoxyhemoglobin, allowing them to capture rich information about multiple parameters related to neurovascular coupling. Other OIS techniques measure blood flow, as in laser speckle imaging (Briers et al., 2013), or changes in scattering related to neural activity (Pan et al., 2018).

Optical imaging can also resolve vascular structure. High resolution measurements of microscopic structural changes with micrometer resolution across several millimeters of cortex can be obtained using ultra-large field two-photon microscopy (Tsai et al., 2015; Lu et al., 2020). This technique can, for example, capture arteriole dynamics that are coherent in related areas across hemispheres (Mateo et al., 2017).

1.3. Fiber photometry

One of the main drawbacks of optical imaging is that it cannot reach deep into the brain (Helmchen and Denk 2005). The advancement of optical imaging has increased the penetration depth of high resolution imaging up to 1–1.2 mm below the surface of the brain (Horton et al., 2013; Liu et al., 2019), but many subcortical structures remain inaccessible. Fiber calcium photometry monitors activity-relevant fluorescence via a fiber optic inserted in tissue where a calcium-sensitive sensor is expressed (Nakai et al., 2001; Adelsberger et al., 2005; Tian et al., 2009; Dana et al., 2019) and is crucial to imaging neuronal activity in areas that are below 1 mm. For instance, the activity of the rat hippocampus, ~2.7 mm below the pial surface, can be measured by first expressing the calcium sensor GCaMP in hippocampal neurons and later measuring their calcium dynamics through fiber optic recordings (Chen et al., 2019). Fiber photometry has lower temporal resolution than electrophysiology and does not allow single cell imaging (Sych et al., 2019) and is compatible with fMRI. Optical fibers are non-ferromagnetic, minimizing disruption to the MR image, and convey signals that are not affected by the rapidly-changing magnetic fields during image acquisition, conferring artefact-free measurements. Most of the signal captured by the fiber derives from $\sim 10^5$–10^6 μm^3 around a 200 μm fiber, although this depends on fibre geometry (Pisanello et al., 2019). Concurrent measurement of the BOLD signal and imaging of neuronal and astrocytic calcium transients was first achieved a decade ago using organic calcium sensors (Schulz et al., 2012) and permits interrogation of the contribution of specific neuronal and astrocytic population to the BOLD signal (He et al., 2018; Wang et al., 2018). The relatively simple fiber photometry technique facilitates combination with other methods along with fMRI, such as optogenetic stimulation (Albers et al., 2018).

1.4. Electrophysiology

While optical imaging has grown more and more powerful in recent years, electrophysiology is still the foundation on which our knowledge of the brain's inner workings rests. Microelectrode recordings of single cell firing rates, multiunit activity (MUA), and local field potentials (LFPs) have provided many of the circuit characterizations

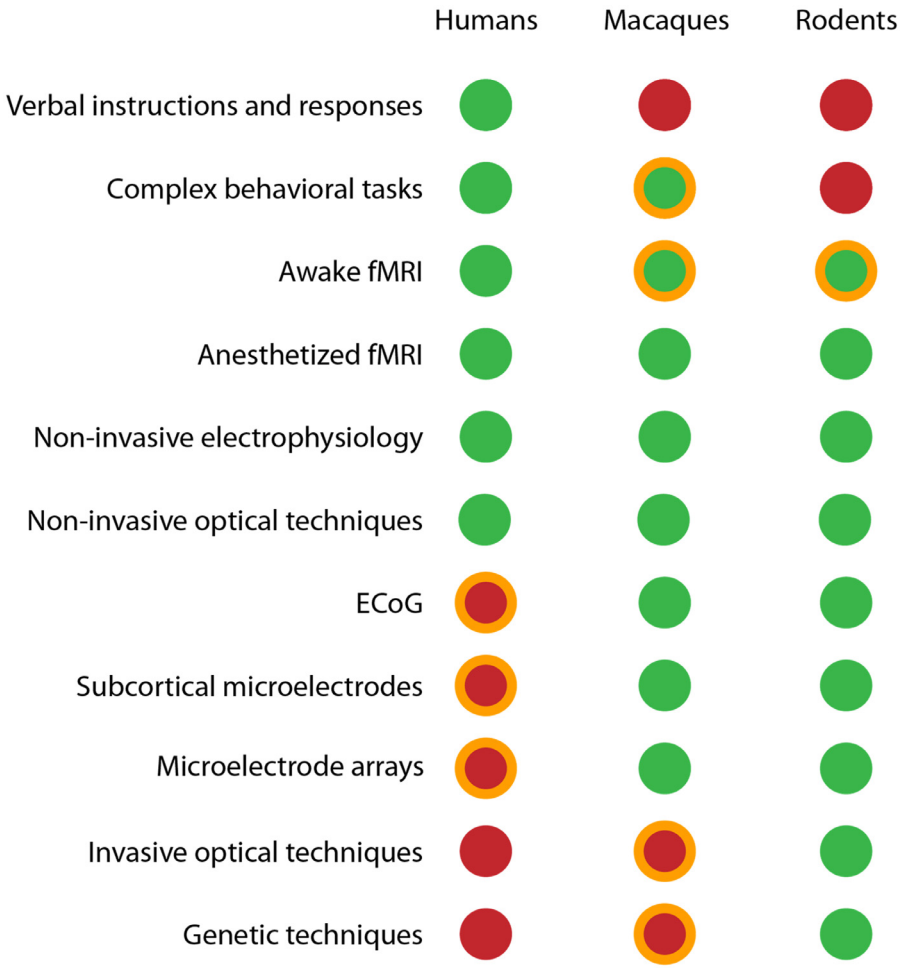

Fig. 1. Currently, no single model organism can accommodate the full range of experimental approaches. Instead, complementary experimental approaches are applied across model organisms. For each model, some approaches are readily applicable (green), some are applicable to an extent (green with orange outline), some are applicable in rare conditions (red with orange outline), and some are inapplicable (red). Only a few common model organisms are shown; others, such as marmosets, are increasingly available and may help to bridge the gap between rodents and large primates (For interpretation of the references to color in this figure legend, the reader is referred to the web version of this article.).

that established the context for the interpretation of rs-fMRI. Simultaneous measurements of neural activity and fMRI have provided insight into the neural basis for the BOLD response (Logothetis et al., 2001; Lu et al., 2007; Magri et al., 2012). While the number of channels available for electrophysiological recording is constantly increasing (Carandini, 2021), simultaneous rs-fMRI and electrophysiology remains limited to a relatively small number of sites, because every additional electrode increases the amount of potential interference between the modalities (Kleinfeld et al., 2019). The technical challenges of combining electrophysiology with MRI include image distortion near the electrodes and unwanted noise in the electrical recordings from currents induced by gradient switching during image acquisition. Electrophysiology can be more easily combined with amperometric measurements of oxygen concentration, which measure the concentration of free oxygen in the tissue. This approach sacrifices the whole brain coverage of rs-fMRI, but provides spatial and temporal resolution of oxygen signals comparable to that of the electrophysiological signals (Bentley et al., 2016; Ledo et al., 2017). It allows for the examination of local coupling between neural activity and oxygen metabolism as well as the coordination of activity and oxygenation across a limited network of sites.

1.5. Functional ultrasound

The recent development of functional ultrasound (fUS) provides another tool for probing the neurophysiology of the BOLD fluctuations (Mace et al., 2011; Osmanski et al., 2014; Dizeux et al., 2019). In many ways, fUS can serve as a surrogate for BOLD, as it is sensitive to the changes in cerebral blood volume and flow (CBV and CBF) that are involved in the BOLD signal. Compared to optical imaging techniques, fUS is able to image much deeper into the brain; however, skull thinning or removal is usually (but not always Manwar et al., 2020) required, acquisition is often limited to a single coronal slice, and some portions of the brain remain inaccessible. fUS of the rodent brain has the advantage of higher spatial and temporal resolution than are typically obtained with rs-fMRI, on the order of 100 μm in plane and up to several ms per image (Osmanski et al., 2014; Dizeux et al., 2019), which poses certain advantages for the investigation of cerebral hemodynamics, especially in the cortex (Urban et al., 2014). fUS is also appealing for studies in unanesthetized animals, as the requirements on animal constraint are less stringent than for MRI, image acquisition is far quieter than MRI, and the imaging system enables more naturalistic environments than the confined space of a preclinical MRI scanner. A recent demonstration of the power of fUS comes from measurements in awake, behaving mice that showed deactivation of the retrosplenial cortex during a sensory task (Ferrier et al., 2020). The retrosplenial cortex has been posited as a key area in the default mode network (DMN) in rodents, but because fMRI studies of behavior are rarely performed in rodents due to the challenges involved, there was no direct evidence that it deactivated during task performance as the DMN does in humans (Fox et al., 2005). fUS is thus perfectly positioned to bridge the gap between rs-fMRI in anesthetized animals and rs-fMRI in awake humans.

Together, these invasive techniques provide a detailed picture of neuronal, metabolic, and hemodynamic processes across a wide range of spatial and temporal scales that cannot be obtained in humans (Fig. 2). The noninvasive nature of MRI makes it the ideal technique to serve as a bridge between these informative experiments in animals and their ultimate application to the interpretation of human neuroimaging studies. In the next sections, we review how animal studies help us to under-

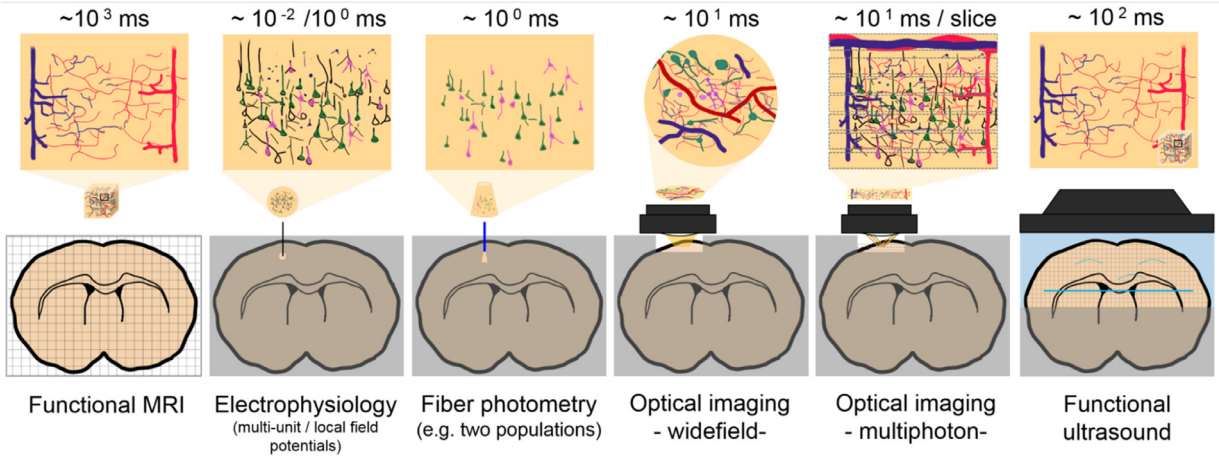

Fig. 2. The figure illustrates six of the most common imaging modalities to measure brain function in rodents. Typical temporal resolutions are shown on the top. The upper panels represent the tissue components that contribute to the recorded signal in each modality: the vasculature, in functional MRI and in ultrasound; all of the neurons surrounding the electrode, in electrophysiology; specific cell types (by using specific promoters), in fiber-based photometry measurements; and all of the tissue components, in microscopy techniques. The panels on the bottom represent the extent of the brain that can be recorded with each technique. While fMRI and ultrasound allow recording of signals from a large portion or even the whole brain, electrode or optical fiber-based measurements are usually restricted to a singular measuring point, and microscopy is limited to superficial portions of the brain. On the other hand, fMRI and ultrasound provide an integrated vascular-based signal from relatively large voxels, while microscopy can identify singular neurons in their particular environment. The spatial resolution of each technique depends on the particular method employed.

stand the link between brain activity and the BOLD response, and then describe insights into the coordination of activity across areas that are obtained from these experiments.

2. Local neural activity and the hemodynamic response

Understanding how local BOLD signal changes are linked to local neural activity is a necessary component of understanding how correlated BOLD fluctuations arise across the brain. Coordination across areas could in principle arise at any segment of the chain of events that constitutes neurovascular coupling, whether from the neural activity itself to a network-level change in metabolic demand to a widespread modulation of vascular tone. A number of reviews of recent work on the links between neural activity and the BOLD response are available (for example, Drew et al. 2020). Here we provide a succinct summary of current thought on the neurophysiology of the BOLD signal to establish a framework for understanding the coordination of neural activity observed with rs-fMRI.

2.1. Excitatory neurons and neurovascular coupling

Neurovascular coupling translates the signal from neurons to microvessels and involves astrocytes, pericytes, endothelial cells and smooth muscle cells. Multimodal experiments have been essential in establishing the coherence of the neurovascular partners during the spontaneous ultra-slow oscillations that are at the core of rs-fMRI (Niessing et al., 2005; Scholvinck et al., 2010; Magri et al., 2012; Ma et al., 2016; Mateo et al., 2017; Winder et al., 2017; Echagarruga et al., 2020). For example, simultaneous mesoscale calcium imaging and intrinsic signal imaging has shown that, on average, neuronal activity typically precedes hemodynamic responses in the resting state condition in the absence of stimulation (Ma et al., 2016; Wright et al., 2017). In a recent technical tour de force, whole brain fMRI was combined with wide-field calcium imaging of the cortical mantle (Lake et al., 2020) to show that one third of the variance in the BOLD signal could be accounted for based on spontaneous excitatory activity. Similarly, simultaneous rs-fMRI and microelectrode recording found that the correlation between LFP power and the BOLD signal was between 0.26 and 0.44, depending on the anesthesia used (Zhang et al., 2019). The correlation coefficients from rs-fMRI are slightly smaller than the value of ~0.6 inferred from two-photon measurements of arteriole diameter concurrent with the LFP (Mateo et al., 2017). These reports provide strong evidence that spontaneous BOLD oscillations are tied to fluctuations of the brain's intrinsic excitatory activity.

Furthermore, multimodal experiments provide insight into the types of activity that are reflected in the BOLD signal. The first simultaneous electrophysiological recordings and fMRI in monkeys showed that the BOLD signal is predicted by synaptic inputs and neuronal firing in the cortex in response to visual input. LFPs, believed to result primarily from synaptic inputs within the area, are actually a better predictor of the BOLD signal (Logothetis et al., 2001) than the local spiking activity in response to visual stimulation. On the postsynaptic side, the gamma band of the LFP is overall the most efficient of bands to predict both the fMRI signal (Logothetis et al., 2001; Niessing et al., 2005; Scholvinck et al., 2010; Magri et al., 2012) and arteriole dilation and oxygenation in the cortex (Mateo et al., 2017; Winder et al., 2017; Echagarruga et al., 2020). The activation of a specific area via optogenetic stimulation of cortical excitatory neurons induces a local BOLD response as well as a BOLD response in contralateral and secondary areas, which defines a functional network (Lee et al., 2010; Desai et al., 2011; Leong et al., 2016).

On the presynaptic side, locally generated spike rates are reflected in the hyperemic response (Lee et al., 2010; Scott and Murphy 2012; Kahn et al., 2013). These responses are not abolished by blocking glutamatergic ionotropic neurotransmission (Scott and Murphy 2012; Kahn et al., 2013; Iordanova et al., 2015), which suggests that local excitatory action potentials have both synaptic and non-synaptic excitatory dilatory effects on the vasculature and therefore both contribute to the BOLD fluctuations.

Potential mechanisms linking excitatory activity and hemodynamics. The release of potassium by neurons during action potentials is a likely candidate to act in neurovascular coupling via generation of a hyperpolarizing pulse by voltage-gated and potassium concentration-sensitive potassium channels. Potassium injections close to a capillary are followed by a hyperemic response in the upstream arteriole, and 80% of this response is abolished by blocking inward-rectifier potassium channel (KIR2.1) *in vivo* (Longden et al., 2017). In a parallel study, potassium-induced dilation was strongly affected by genetically ablating KIR2.1 only in endothelial cells in a knock-out mouse. This puts endothelial cells as sensors of neuronal activity in a position to con-

trol upstream blood flow and meet the oxygenation needs of the active area.

Cyclooxygenase-2 (COX-2), which is expressed by cortical excitatory neurons (Lecrux et al., 2011) is another contributor to neurovascular coupling. In brain slices, there is pharmacological evidence that in response to neuronal activation, COX-2 permits prostaglandin E2 increases that target receptors potentially on smooth muscle (and pericyte) cells that participate in the dilation (Lacroix et al., 2015). Using COX-2 inhibitors dramatically decreases the local hemodynamic response to optogenetic stimulation of excitatory neurons without abolishing it. Although optogenetic stimulation offers a way to activate a specific group of cells, the postsynaptic recruitment of inhibitory neurons is much faster (i.e., milliseconds) (Mateo et al., 2011) than the hemodynamic responses (i.e., seconds), and as a result, in the absence of synaptic blockers, the hemodynamic responses to excitatory and inhibitory neurons are then mixed and part of the response may come from the postsynaptic activation of vasoactive inhibitory neurons.

2.2. Inhibitory neurons and neurovascular coupling

Cortical inhibitory neurons are a diverse population with different expression patterns and morphologies (Gonchar et al., 2007; Petilla Interneuron Nomenclature et al., 2008; Perrenoud et al., 2012; Kubota et al., 2016; Tremblay et al., 2016), yet all release the neurotransmitter GABA. In the cortex, only 20% of neurons are inhibitory neurons (Kim et al., 2017; Torres-Gomez et al., 2020). They fire at higher rates than excitatory neurons and their activity is modulated across brain states and behavioral tasks (Gentet et al., 2010; Niell and Stryker, 2010; Gentet et al., 2012; Liguz-Lecznar et al., 2016; Urban-Ciecko and Barth, 2016), making them plausible contributors to the spontaneous BOLD fluctuations observed with rs-fMRI.

Studies in brain slices show that relatively slow arteriole dilations can be elicited by the excitation of a single interneuron that expresses vasoactive intestinal peptide (VIP) or nitric oxide synthase (NOS). Neuropeptide Y (NPY) expressing interneurons induced constriction and somatostatin (SOM) expressing interneurons could elicit both constrictions and dilations (Perrenoud et al., 2012), indicating a possible role for inhibitory activity in neurovascular coupling corresponding to the effect of their vasoactive components.

The optogenetic stimulation of inhibitory neurons regardless of their subtypes induces large arteriole dilation similar to that of sensory responses, followed by an NPY-mediated undershoot (Uhlirova et al., 2016) and CBF increase (Anenberg et al., 2015; Vazquez et al., 2018). After a blockade of synaptic transmission, the hemodynamic responses to optogenetic stimulation were barely affected, but when using a NO blocker, 75% of the response was abolished, leading to the hypothesis that the hemodynamic effects are mediated directly by NOS neurons (Vazquez et al., 2018; Krawchuk et al., 2020). Inactivation of NOS neurons using designer receptors exclusively activated by designer drugs (DREADDs) shows a decoupling of neuronal activity with arteriole diameter (Echagarruga et al., 2020) and local oxygenation as seen with OIS (Lee et al., 2020). Interestingly, parvalbumin neuron (PV) stimulation induced arteriole constriction (Urban et al., 2012) and negative BOLD signal (Lee et al., 2010; Lee, Stile et al., 2021). All of the manipulations cited are very artificial and only establish causal links. Optogenetic stimulation of inhibitory neurons led to a biphasic BOLD signal locally at the stimulation site followed by negative downstream BOLD (Moon et al., 2021). Of note, the HRF that arises from stimulation of inhibitory neurons appears to be highly variable on the stimulation frequency when compared to the activity of excitatory neurons (Moon et al., 2021). In order to understand better the physiological role of inhibitory neurons during spontaneous activity, in the future we need to perturb and/or record the activity of subtypes of inhibitory neurons concurrently with vasodynamics and the release of vasoactive compounds using genetically encoded sensors (Oh et al., 2019; Pal and Tian 2020).

2.3. Astrocytes, pericytes, and neurovascular coupling

The study of the role that astrocytes play in neurovascular coupling is a shining example of how the refinement of imaging and stimulation techniques furthers the understanding of the role of cell types in neurovascular coupling (Cauli and Hamel 2018). At the ultra-slow frequencies (< 0.3 Hz) detected with rs-fMRI, vascular fluctuations are coherent with neuronal fluctuations but not with astrocytic activity fluctuations (Gu et al., 2018). Despite the lack of coherence with vascular fluctuations, optogenetic stimulation of astrocytes triggers a positive BOLD signal without changing neuronal activity (Masamoto et al., 2015; Takata et al., 2018), so it is clear that they have the capacity to impact the vasculature. In more physiological conditions, astrocytic calcium in the cortex increases at the soma and in processes in response to sensory stimulations (Nizar et al., 2013; Tran et al., 2018). However, these increases are delayed relative to the onset of vasodilation, therefore calling into question the role of astrocytes in the physiological initiation of the dilation. In the olfactory bulb, on the other hand, calcium transients in astrocytic endfeet precede the vasodilation (Otsu et al., 2015). Pathways that bridge the astrocytic activity and vasodynamics are under study and suggest a series of molecular candidates. As an example, astrocytes can act directly onto the pericytes (Mishra et al., 2016).

Brain pericytes are contractile cells (Fernandez-Klett et al., 2010) that wrap around capillaries and precapillary arterioles (Hartmann et al., 2015). Optogenetic stimulation of pericytes can trigger vessel constriction and decrease the blood flow in some small vessels (Attwell et al., 2016; Nelson et al., 2020; Grubb et al., 2021; Hartmann et al., 2021). The control of capillary diameter by pericytes in physiological conditions is at the center of an important debate (Hill et al., 2015; Attwell et al., 2016) as their position is ideal to generate small changes in capillary diameter that have a dramatic effect on blood flow (Blinder et al., 2013). Pericytes exhibit spontaneous calcium transients that are sensitive to neuronal activity (Rungta et al., 2018) and they are likely involved in maintaining basal vascular tone (Hartmann et al., 2021).

While we are beginning to understand how excitatory neurons, inhibitory neurons, astrocytes and pericytes might separately contribute to the BOLD fluctuations, the complex interplay between these different types of cells that exists during normal brain function remains insufficiently understood, and is at the frontier of research into neurovascular coupling.

2.4. Neurovascular coupling outside of sensory cortical areas

The majority of the work on neurovascular coupling has been performed in primary sensory cortex, for the simple reason that activity can easily be elicited with the proper sensory stimulus, and the timing of the activity can be precisely controlled. A few studies have examined neurovascular coupling in areas outside of the sensory cortex, with sometimes conflicting results. Particularly in rodent models of epilepsy, localized reductions in the BOLD signal have been observed despite increases in neural activity. David et al., observed deactivation in the striatum during spike wave discharges while activation was present in the somatosensory cortex and the thalamus (David et al., 2008). Similarly, Mishra et al. (2011) found that cerebral blood volume (CBV), cerebral blood flow (CBF), LFP, MUA and the fMRI signal in somatosensory cortex and the thalamus all increased during spike wave discharges, while in the striatum, the fMRI signal and hemodynamic metrics decreased despite an increase in LFP and MUA (Mishra et al., 2011). Such atypical neurovascular coupling was reported in studies using noxious forepaw stimulation in the rat, which increases LFP, MUA, and c-Fos activity (Shih et al., 2009) and produces negative BOLD, CBF and CBV signals in the striatum (Shih et al., 2009, 2011, 2014). Deep brain stimulation of striatal output areas – a procedure known to induce antidromic striatal activation - similarly results in CBV decreases in the striatum (van den Berge et al., 2017). Using electrophysiology, pharmacology, and

CBV-weighted fMRI in healthy and dopamine-depleted rats, Shih et al. showed that the negative striatal hemodynamic response is related to the unique endogenous neurotransmission in the (Shih et al., 2009). In another study, in rats with generalized seizures induced by bicuculline injection, BOLD deactivation was observed in the hippocampus while activation was present in the cortex. A thorough examination of neural activity, oxygen metabolism, and blood flow determined that while blood flow and oxygen metabolism increased in both the hippocampus and the cortex, neural activity in the hippocampus during the seizure increased 1000-fold, compared to a 100-fold increase in the cortex, and thus the balance between neural activity and hemodynamics resulted in a negative BOLD signal (Schridde et al., 2008).

Another study using multielectrode arrays, OIS, and fMRI in the rat examined the neurovascular coupling in different areas of the ascending vibrissa pathway during vibrissa stimulation, and found that some areas exhibited a nonlinear or even inverse relationship between neural activity and hemodynamics (Devonshire et al., 2012). Even non-sensory cortical areas may have neurovascular coupling that differs from the typical model. In head-fixed but awake mice, it was found that locomotion induced neural activity in somatosensory cortex that was accompanied by an increase in CBV, but while neural activity also increased in frontal cortex, the CBV was unchanged (Huo et al., 2014). As an interesting potential mechanism, locomotion increases extracellular potassium (Rasmussen et al., 2019), which could potentiate hyperpolarization of the vascular endothelium in response to local neuronal activity (Longden et al., 2017). These studies serve as a warning that blithe application of the same hemodynamic response function in all areas of the brain could provide a distorted view of underlying neural activity. Further investigation of neurovascular coupling in areas outside of the sensory cortex is needed to give guidance about areas and conditions where neurovascular coupling is likely to be altered.

2.5. Spatial specificity of the hemodynamic response

In addition to the underlying interplay of neurons, astrocytes, vascular components and diverse metabolites that results in the BOLD response, it is important to also consider the spatial specificity of fMRI functional mapping, which is intrinsically limited by the nature of the fMRI signal, i.e. the neurovascular coupling that transfers the neural signal to the cerebrovasculature (Kozberg and Hillman 2016). The perfusion domain consists of a penetrating arteriole that supplies oxygenated blood to a patch of cortex, a convoluted network of capillaries that distributes the oxygenated blood, and a penetrating venule that collects the deoxygenated blood and drains into the venous system (Blinder et al., 2013). In rodents, the approximate distance between penetrating venules is ~200 μm (Nishimura et al., 2007), which can reach up to ~1 mm in humans (Cassot et al., 2006; Weber et al., 2008; Adams et al., 2015; He et al., 2018; Uludag and Blinder, 2018). Numerous studies of the spatial specificity of fMRI have tried to identify the spreading of the fMRI contrast (e.g. the BOLD effect) across the vessel architecture from the active neuronal site. In an attempt to approximate the maximum distance at which one could measure oxygenation changes derived from neuronal activation, Turner (2002) took into consideration the diameter of a pial vein and its distance to its most distal branches. It was estimated that a 100 mm^2 cortical area, which could theoretically be drained by a single pial vessel, could produce blood oxygenation changes up to a radius of 4.2 mm, setting an upper limit for the hemodynamic changes derived from activation of a cortical patch (Turner 2002).

Columnar specificity. Experimental methods to quantify the spatial specificity of fMRI rely on comparing the vascular signals and the true neuronal responses. In humans, the estimation of true neuronal responses relies on knowledge of the underlying neuroanatomy, rather than direct measurements. For instance, a non-invasive approach consists of measuring ocular dominance columns with fMRI and comparing the size of these columns with reference columns in an *ex vivo* histochemistry-based atlas. In a human fMRI ocular dominance study, the full-width at half-maximum (FWHM) of the hemodynamic PSF was estimated to be 0.86 mm for spin-echo BOLD and 0.99 for gradient-echo BOLD (Chaimow et al., 2018), which suggests that the FWHM of the true hemodynamic PSF lies well below 0.8 mm, as fMRI measures are contaminated, to a certain degree, by motion-derived blurring, among others.

In animal models, it is possible to measure neural activity directly. One study combined high resolution fMRI (270 μm by 279 μm in plane) with a microelectrode array to measure neuronal activity in the somatosensory cortex of non-human primates (Shi et al, 2017). They showed comparable activation extents of columnar responses, demonstrating the capability of BOLD fMRI to accurately map neuronal activation during stimulation and at rest. Another study used a combination of optically-based CBV measurements, laser doppler flowmetry CBF measurements, and electrophysiological recordings in mice to assess optogenetically-evoked neuronal and hemodynamic responses in the somatosensory cortex (forelimb), to show that the PSF of the hemodynamic response spans approximately 175 μm (Vazquez et al., 2014). The strong resemblance between the general spatio-temporal features of columnar units investigated with fMRI and those measured with electrophysiology supports the use of fMRI to extend the investigation of cortical networks.

The temporal dynamics of the BOLD response can be leveraged to improve spatial specificity. By selectively mapping the initial dip of the hemodynamic response voxel-wise, iso-orientation columns in the cat primary visual cortex could be distinguished with fMRI (Kim et al., 2000; Fukuda et al., 2006). A similar approach that differentiates between early and late responses has been used to identify micro vs. macrovasculature activation, which can greatly reduce the vascular bias observed in evoked laminar fMRI (Kay et al., 2019, 2020).

At extremely high spatial resolution, it becomes possible to distinguish individual penetrating vessels using high-field T2*-weighted methods for rodent fMRI (Yu et al., 2016, He et al., 2018, Chen et al., 2019). This allows vessel-specific BOLD or CBV signal to be identified from penetrating arterioles and venules (> 20–70 μm in rodents) and pushes up against the limits of the theoretically-possible specificity of the BOLD signal (Fig. 3). These studies raise a new aspect to be considered when interpreting high-resolution columnar results: the functional identification of single vessels with high-field fMRI mapping and the distinct connectivity patterns identified in venous and arterial networks suggest that vessel distribution is a critical factor in columnar BOLD fMRI.

Laminar specificity. The specificity of the BOLD signal as compared to the size of a cortical column arrives at an estimate of the PSF across the cortical sheet, i.e., tangential plane. Also of interest is the specificity of BOLD in the orthogonal direction, i.e., radial plane, across the layers of the cortex. The cortical thickness can be divided into layers of different cyto- and vaso- architecture (Duvernoy et al., 1981; Palomero-Gallagher and Zilles 2019). The largest vessels, pial arteries and veins, run tangentially over the surface of the cortex, smaller vessels penetrate into the cortical depths radially, and a slightly but significantly anisotropic capillary mesh exists within the cortical ribbon, the density of which varies across the cortical depth (Weber et al., 2008; Ji et al., 2021). Instead of measuring across quasi-discrete neurovascular units as in studies of tangential specificity, estimates of radial specificity must disentangle layer-specific input from the complex vascular organization, which includes the draining effect of ascending venules that contaminate the upper layers with blood from deeper territories.

Given the complex neurovascular coupling features and different laminar-specific metabolic demands (Borowsky and Collins, 1989; Weber et al., 2008; Devonshire et al., 2012; Blinder et al., 2013; Shih et al., 2013; Urban et al., 2014), the interpretation of BOLD fMRI across cortical layers remains one of the most challenging and interesting topics of fMRI. Despite the complexity of the laminar environment in the cortex, multiple studies have proven the capa-

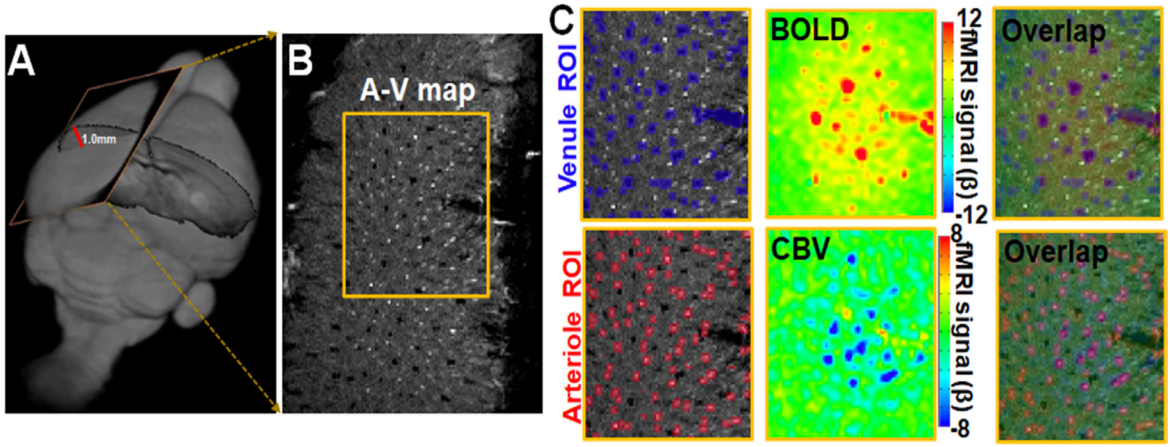

Fig. 3. Single-vessel mapping with fMRI. A. The 3D contour of a rat brain shows the 2D slice perpendicular to the penetrating vessels, which covers one hemisphere for single-vessel fMRI mapping. B. The integrated multi-gradient-echo (MGE) image shows the arteriole-venule (A–V) map with arteriole voxels as bright dots and venule voxels as dark dots (yellow box: forepaw somatosensory cortex, FP-S1). C. The venule-specific BOLD fMRI and arteriole-specific CBV fMRI functional maps are overlaid on the A–V maps (venule ROI in blue, arteriole ROI in red). Adapted from Yu et al. (2016) (For interpretation of the references to color in this figure legend, the reader is referred to the web version of this article.).

bilities of high-resolution fMRI to reliably track activation changes across the cortical thickness in both bottom-up and top-down tasks (Silva and Koretsky, 2002; Goense and Logothetis, 2006; Yu et al., 2014; Poplawsky et al., 2015; Siero et al., 2015; Huber et al., 2017; Kashyap et al., 2018; Finn et al., 2019; Sharoh et al., 2019), and combined laminar fMRI with EEG revealed frequency-specific modes of communication at different cortical depths, e.g., superficial layers positively correlated with gamma oscillations but deeper layers more involved with beta activity (Scheeringa et al., 2016), in agreement with laminar LFP studies (Buffalo et al., 2011). The growing body of literature on high-resolution fMRI with multi-modality studies to target a diverse series of structures in the micro-to-mesoscale levels demonstrates the potential of fMRI to sample brain function with great accuracy and supports the ambition to map laminar, columnar and vascular networks with fMRI.

3. Coordination of intrinsic activity across the brain

Understanding how neurovascular coupling leads to hemodynamic fluctuations that follow fluctuations in intrinsic neural activity gives us a partial picture of the origin of the coordinated BOLD fluctuations observed with rs-fMRI. To understand how neural activity and hemodynamics are coordinated across areas, multisite, multimodal measurements are essential.

Conceptually, there are a number of ways that activity could be coordinated that are consistent with known neuroanatomical and neurophysiological processes (Fig. 4). The simplest explanation is that areas that are directly connected, whether via long range white matter tracts or collateral projections, tend to activate together. Similarly, two areas that receive direct input from a third area, i.e., common input, would exhibit correlated activity with each other and with the third area. These connectivity-based interpretations are the basis for the vast majority of rs-fMRI analyses, yet they may provide an overly-simplistic view of the complex system that is the brain. From the perspective of nonlinear dynamics, the coordination of intrinsic brain activity could arise from interactions between local populations of neurons connected via a vast structural network to produce patterns of “network” activity that are not immediately obvious based on structural connections alone. For example, it is difficult to explain the anticorrelation observed between certain networks based on direct connections alone, but it arises naturally in models based on the full structural network of the brain (Cabral et al., 2011).

While there is still much to learn about the functional architecture of the brain, a few principles seem likely to govern the brain’s structure and resulting patterns of activity. The minimization of metabolic costs implies certain wiring rules (van den Heuvel and Sporns, 2011; Bullmore and Sporns, 2012; Betzel et al., 2016; Liang et al., 2018) and operational levels of activity (Tagliazucchi et al., 2012, Haimovici et al., 2013). The vasculature has co-evolved with the metabolic needs of the brain (Ji et al., 2021), and as a result, the densely interconnected core areas of the brain are also highly perfused (Liang et al., 2018), and the vasculature may be regulated in such a way as to support functional networks (He et al., 2018, Bright et al., 2020).

Given the various factors that contribute to coordinated brain activity, how can we decide which ones are dominant? Time-averaged measures like correlation provide a single snapshot of how activity is coordinated over relatively long periods of time, but more recently-developed analysis methods that provide time-varying estimates of activity and/or coordination can give deeper insight into processes that are likely to contribute. Different analysis methods are sensitive to changes in activity that occur at different time scales. For example, point process analysis and coactivation patterns can capture changes that persist for only a single TR (Liu and Duyn, 2013; Petridou et al., 2013). Sliding window correlation and brain states obtained from clustering sliding window time courses are sensitive to slower changes in activity determined by the length of the window that is used (Allen et al., 2014; Shakil et al., 2016). Some methods identify repeated patterns, e.g., quasiperiodic patterns (Majeed, et al., 2011; Yousefi et al., 2018) or common transitions of activity across brain states or between areas (Chen et al., 2016; Vidaurre et al., 2017).

In the next section, we review mechanisms for different processes that might guide coordinated activity and evidence that they contribute to the brain’s functional organization, using both time-averaged and time-varying analysis techniques along with multimodal experiments.

3.1. Functional connectivity and direct white matter connections

3.1.1. Similarity of structural and functional connectivity

Correlated activity in two physically separated brain areas is often interpreted as arising from direct white matter connections between those areas. White matter tracts not only connect different cortical regions but also sustain broad subcortical projections from deep brain functional nuclei to the cerebral cortex (Wycoco et al., 2013). Many areas that exhibit correlated BOLD fluctuations do have direct connections, and the matrix of structural connectivity within the brain as measured with

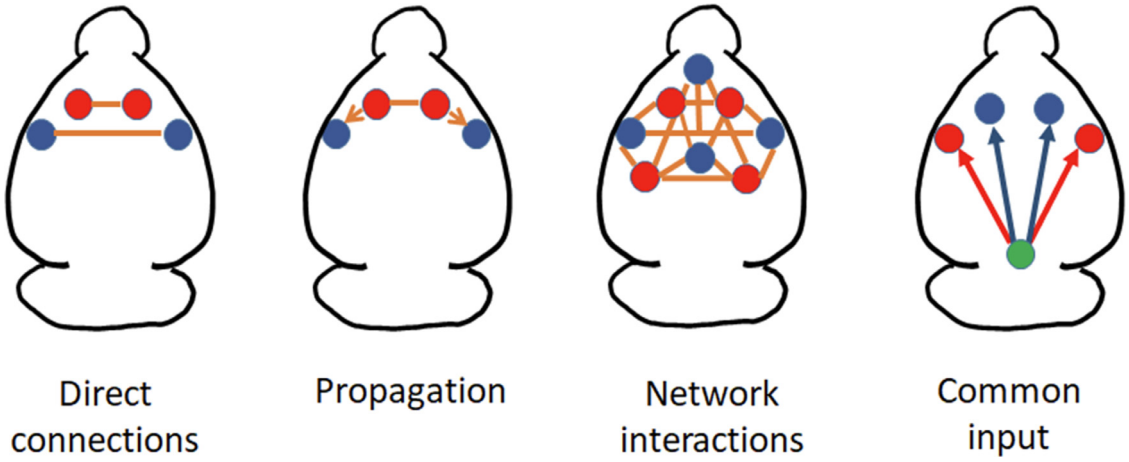

Fig. 4. Networks of correlated BOLD fluctuations could arise from multiple mechanisms. In the first panel, two bilateral networks (one red, one blue) are driven by separate, direct white matter connections. This scenario is the simplest and functional connectivity is often interpreted to reflect direct connections as a first approximation. In the second panel, correlations in the red network arise via a direct white matter connection. Activity propagates over time along the cortex to the blue areas, which appear to be correlated despite the lack of a direct connection. In the third panel, the red areas and blue areas are part of a larger network. Correlations within each subnetwork and anticorrelation between the subnetworks arises through the interactions of activity over the entire structural network. The fourth panel shows another scenario, where red areas and blue areas are both driven by input from a single area, representing neuromodulation. Differences in receptor type and density may account for different responses to the neuromodulatory input in red and blue networks. It is likely that all of these mechanisms contribute to functional connectivity (For interpretation of the references to color in this figure legend, the reader is referred to the web version of this article.).

diffusion-based tractography or viral tracing techniques has substantial similarity to the matrix of functional connectivity; the correlation between structural and functional connectivity is ~0.2–0.4 for an individual in the HCP dataset (Messe, 2020). Unimodal areas and particularly visual cortex exhibit tighter coupling between structural and functional connectivity than transmodal areas (Vazquez-Rodriguez et al., 2019). Nevertheless, some areas that exhibit strong correlation in rs-fMRI are connected only via indirect pathways, complicating this interpretation of functional connectivity. One contributing factor is that typical MR-based methods of mapping structural connectivity have certain biases and do not capture some types of connections well, which could account for some of the differences between structural and functional connectivity (Reveley et al., 2015; Schilling et al., 2018; Yeh et al., 2020). For example, diffusion based tract-tracing methods are more sensitive to terminations in the gyral crown than in sulci (Schilling et al., 2018), and long range connections are underestimated (Reveley et al., 2015).

In mice, injection of anterograde tracers in multiple areas of the cortex has allowed the production of a highly detailed structural connectivity atlas (Allen Mouse Brain Connectivity Atlas; Oh, Harris et al. 2014). However, even in animal models where viral tracers can be employed instead of MR-based methods, structural connections explain a limited number of the functional connections that are observed. In the rat, a meta-analysis of tracing data combined with rs-fMRI found a group level Spearman's correlation of 0.48 between the structural and functional connectivity matrices (Diaz-Parra et al., 2017). In marmosets, connectivity measured with retrograde tracer injections was correlated with functional connectivity between areas ranging from -0.1 to 0.6 after controlling for the effects of the distance between two brain regions (Hori et al., 2020). While viral tracers have their own biases, the moderate similarity observed between functional and structural connectivity for any tract-tracing method suggests that direct white matter connections provide only a partial explanation for the coordination of activity across the brain (Kura et al., 2018). Nevertheless, recent studies that use dense whole-brain tracing combined with rs-fMRI are providing new insights into the potential mechanisms of network organization. The extensive characterization of the mouse structural connectome in combination with mouse rs-fMRI has recently offered a plausible explanation for the way brain networks work and interact with each other (for instance, see Colettaet al. 2020).

3.1.2. Relationship between BOLD and neural activity in areas connected directly via white matter pathways

The interhemispheric connections that travel through the corpus callosum connect homologous areas in the left and right hemispheres, which generally exhibit strong, and largely symmetric, functional connectivity as well. These areas have been the target of many experiments involving simultaneous microelectrode recording and rs-fMRI or wide-field optical imaging of neural activity, which clearly show that neural activity in both cerebral hemispheres is correlated with spatial specificity similar to that seen in the hemodynamic response (Lu et al., 2007; Mohajerani et al., 2010; Pan, Thompsonet al., 2011; Ma et al., 2016). For instance, Ma et al., demonstrated the use of wide-field optical imaging to measure calcium-based neuronal activity (GcaMP fluorescence) concurrently with hemodynamic signals from much of the cerebral cortex in mice (Ma et al., 2016), which allowed a reliable examination of the neurovascular coupling in bilateral areas during wakefulness and under anesthesia.

Most electrophysiological recordings are focused on relatively high frequencies (1 Hz and above). In contrast, the BOLD fluctuations fall mostly below 0.1 Hz (Cordes et al., 2001). The disparity in frequencies complicates comparison across modalities and is usually addressed by filtering and downsampling the electrophysiological data. However, it is also possible to measure very low frequency electrical signals that are comparable in frequency to and coherent with the BOLD fluctuations (Pan et al., 2013). The correlation between these infraslow electrical oscillations and the BOLD signal is at least as strong as the correlation between BOLD and bandlimited power in higher frequency ranges. This correlation between modalities is localized to the area near the electrode and to the comparable area in the other hemisphere, suggesting that infraslow electrical activity could facilitate network communication. In humans, comparable findings have been obtained using EEG (Hiltunen et al., 2014; Grooms et al., 2017).

Little is known about infraslow electrical activity. One possibility is that the envelope of higher frequency activity is rectified by nonlinear membrane processes and then contributes to the LFP (Ahrens et al., 2002; Haufler and Pare, 2019). Some studies suggest that these slow potentials reflect modulation of cortical excitability (Rockstroh et al., 1993; Rosler et al., 1997), which is consistent with findings using electrocorticography (eCoG) in humans that the low frequency modulation

of both gamma power and firing rate are correlated across hemispheres (Nir et al., 2008). He et al. (2008) found that the slowest eCoG potentials (0.1 - 4 Hz) had a similar correlation structure to the BOLD signal across hemispheres, but that the relationship with gamma band power was state-dependent. Further support for a neural origin comes from Chan et al. (2015) who found that infraslow EEG power was attenuated by the application of drugs that decrease cortical excitability and glutaminergic transmission.

In the more traditional EEG frequency bands above 1 Hz, the precise frequencies of neural activity that best predict BOLD correlation depend on the anesthetic condition, but are not necessarily the frequencies most linked to the local BOLD response. For example, under isoflurane, BOLD correlation between left and right somatosensory cortex is best predicted by the correlation of delta and theta band-limited power of local field potentials from the two areas, while the local BOLD response was linked to broadband power, with a particularly high correlation to power in the beta and gamma bands (Pan et al., 2011). Lu et al., observed a similar relationship between functional connectivity and power coherence in the delta band in rats under alpha-chloralose anesthesia (Lu et al., 2007). In contrast, the highest correlations with the local BOLD signal were observed in high frequency power (gamma band or above) during visual stimulation (Logothetis et al., 2001) or during spontaneous activity (Shmuel and Leopold, 2008).

There are non-neuronal sources of infraslow electrical activity that confound ECoG measurements (Drew et al., 2020). These include astrocytes (Kuga et al., 2011), an intriguing possibility given their links to the vasculature, and changes in the blood-brain barrier potential (Voipio et al., 2003). In the same frequency range, oxygen polarography measurements in four sites from two different networks (visual and DMN) in monkeys showed that correlation peaked at 0.06 Hz and was stronger for sites within the same network than for sites in different networks, providing independent support for a possible infraslow coordination of activity across the brain (Li et al., 2015).

3.1.3. Insights from time-varying analysis of directly-connected areas

Dynamic analysis provides further insight into the relationship between neural activity and BOLD correlation in directly connected areas. In left and right primary somatosensory cortex of rats anesthetized with isoflurane, sliding window correlation of bandlimited LFP power is correlated with sliding window correlation of the BOLD signals from the two areas (Thompson et al., 2013), particularly in theta, beta and gamma bands. Compared to Pan et al. (2011), where time-averaged correlation in the theta and delta bands was most predictive of coordinated neural activity, this suggests that analyses that capture the time-variance of the signal might increase sensitivity to high frequency activity. In humans, sliding window correlation shows there are periods when functional connectivity closely matches anatomical connectivity, and others when functional connectivity is dominated by inter-network interactions (Liegeois et al., 2016).

In wide-field optical imaging, the pattern of bilateral fluctuations changes much more quickly than could be captured by BOLD fluctuations, evolving through different bilateral activity patterns over the course of a few hundred milliseconds (Mohajerani et al., 2010). As in humans, the patterns of spontaneous activity often resemble those evoked by a task or stimulation (Smith et al., 2009; Mohajerani et al., 2013). Chan et al., showed that infraslow cortical activity recapitulates similar motifs to those observed at higher frequencies, a vivid demonstration of how activity can nest across temporal scales (Chan et al., 2015). Parallel work in humans shows that EEG-resolved micro-states that persist for less than one second resemble the spatial patterns of fMRI-defined resting state networks (Custo et al., 2017; Rajkumar, 2021). Similar resting state networks can be detected in OIS measurements of hemodynamics, further support for tight coupling between coordinated neural activity and correlated BOLD signals (Kura et al., 2018).

3.1.4. Effects of white matter disruption on functional connectivity

One way to test the effects of direct connections on functional connectivity is to manipulate the network structure or function by physical or chemical lesions. For example, chemogenetic inhibition of the anterior cingulate cortex (ACC), a key brain hub, reduces functional connectivity across much of the brain (Peeters et al., 2020). Another study in rats found that after callosotomy, both functional connectivity and coherent gamma band power between left and right somatosensory cortex decreased (Magnuson et al., 2014). Similarly, in acallosal mice, the bilateral symmetry of activity mapped with voltage sensitive dye was greatly reduced (Mohajerani et al., 2010). Moreover, the coherence of ultra-slow oscillations of arteriole diameters (0.1 Hz) in related areas across hemispheres depends on the integrity of the corpus callosum (Mateo et al., 2017). These studies support a role for direct connections via the corpus callosum in mediating functional connectivity, but interpretation remains somewhat ambiguous since acallosal mice necessarily adapt for the lack of the corpus callosum during development, and the acute callosotomy procedure used in the rat study is highly invasive and traumatic. Side effects from the surgery may explain why the left and right caudate, which are not directly connected via the corpus callosum, also exhibited reduced functional connectivity after callosotomy. On the other hand, the reduced functional connectivity in the caudate could also be interpreted as a downstream effect of the disruption of coordinated input from the cortex, which would normally drive correlated activity in the caudate.

3.2. Functional connectivity as a consequence of the structural network

One can expand the question of whether functional connectivity arises from direct white matter connections to include the effects of the entire structural network, including feedback loops. In this case, coordinated BOLD fluctuations could arise from the complex dynamics of activity as local neural populations interact with the rest of the brain via the structural network. This type of network interaction can explain some of the correlation that is observed between regions that are not directly connected themselves, and it can account for anticorrelation between certain areas or networks, which is difficult to understand in terms of direct connections alone.

The effects of network structure are typically examined using brain network models, which combine a structural matrix obtained from diffusion-weighted MRI or viral tracing with neural mass models that describe the activity at each brain node. The activity at each node over time is determined by its prior activity and the input from the nodes to which it is connected. A number of different neural mass models have been used, e.g., for a review, see Cabral et al. (2017), all of which require optimal fitting of a number of parameters to find those that give the best fit to measured functional connectivity. Most brain network models recapitulate some aspects of time-averaged functional connectivity but fewer aspects of time-varying functional connectivity (Kashyap and Keilholz, 2019). At this stage of their development, brain network models show that particular network interactions between neural populations can give rise to features that are observed in rs-fMRI data, but the similar performance of a wide variety of models and parameterizations means that they are less successful at eliminating particular conceptualizations of how the brain works.

3.3. Role of intracortical connectivity and propagation

In addition to relatively long range connections via white matter tracts, the cortex is densely interconnected through collateral fibers. These fibers provide another route for coordination of activity across the brain and can account for some of the network structure observed as functional connectivity (Atasoy et al., 2016).

3.3.1. Anatomical structure of cortico-cortical connections

Analysis of structural connectivity in the mouse has demonstrated that axons connecting two cortical areas of the same hemisphere start in the upper and deeper layers of the cortex, run along layer 6, and terminate either in the middle layers of primary cortices or in superficial layers of higher order cortical areas (Watakabe and Hirokawa, 2018). Of the six layers that make up the neocortex (Baillarger, 1840; Palomero-Gallagher and Zilles, 2019), layer 5 accounts for most intra- and inter-hemispheric intracortical (and corticofugal) outputs, and in turn receives inputs from layers 2/3, 4 and 6. Layer 4 is primarily associated with feed-forward projections, e.g., thalamic afferents, while layers 5 and 6 have been observed to play a role in both feed-forward and feedback processes (Douglas and Martin, 1991; Sherman and Guillery, 2011, Tong et al., 2013; Harris et al., 2019). In contrast to the primarily vertical orientation of fibers in other layers, the vast majority of fibers in layer 1 are horizontal or oblique (Palomero-Gallagher and Zilles, 2019), which suggests a role in cortico-cortical connectivity and information processing.

Analyses of structural connectivity atlases in several species suggest that the degree of intra-hemispheric connectivity primarily depends on the distance between targets, while other features, such as the cyto-architectonics, i.e., the dominating cell types, play an important role in both ipsi- and contra-lateral connections (Ercsey-Ravasz et al., 2013; Beul et al., 2017; Goulas et al., 2017; Schmidt et al., 2018). An example can be found in mice, where the granularity of the cortex largely conditions the structural connectivity between distant cortical areas (Goulas et al., 2017). Interestingly, cholinergic projections from the basal forebrain target cortical laminae in a fiber age-dependent manner (Allaway et al., 2020). Anatomical studies, accomplished at least partially *ex vivo* at the microscopic level, provide the hard-wiring model for potential cortical connections; however, exploring the true functional connectivity requires *in vivo* techniques such as electrophysiology, to reliably detect neuronal activity within the cortex, or rs-fMRI, to assess the coordination, e.g., temporal correlation, between areas.

3.3.2. Propagation of evoked activity through cortico-cortical connections

Despite their invasiveness, electrophysiology studies can provide reliable detection of neuronal activity with both laminar- and columnar-specificity, identifying the spreading of information flowing through the cortex. For instance, recording from electrodes placed along the cortical depth in mouse M1 during optogenetic stimulation demonstrated cortical depth-dependent activation upon stimulation of different areas, e.g. the orbital cortex activated neurons in layer 6, secondary motor cortex activated layer 5b neurons, and thalamic and primary somatosensory cortex (S1) stimulation targeted mainly upper layers (Hooks et al., 2013), demonstrating the differential role of neurons across the cortical depth to maintain connections across distant areas. Cortical columns add an important dimension to the study of functional networks with high specificity. Although cortical columns have been regarded as the smallest unit in the cerebral cortex (Horton and Adams, 2005), inter-columnar interactions are critical to shape receptive fields, hence, the autonomy of a single functional column is questionable, as interactions between neighbors are needed for proper operation (Lund et al., 2003). For example, excitatory neurons of the cortex are usually inhibited by interneurons within the same cortical lamina but in a different column. Lateral inhibition from neighboring intra or inter-laminar neurons (Katzel et al., 2011) provides a mechanism to shape or restrict neuronal receptive fields.

The sophisticated organization of the cerebral cortex in laminae and columns suggests that cortical networks spreading across multiple cortical areas result from a complex interplay at a mesoscale (Mitra, 2014; Roe, 2019). Although this dimension is better explored with multi-site electrodes, broad networks expanded across multiple brain areas require imaging techniques that can cover big fields of view; hence, fMRI has been largely used to characterize inter-areal interactions and novel high-resolution fMRI methods are starting to bridge the gap between high-resolution electrophysiology and large-coverage fMRI mapping. For instance, using a 7T scanner, Huber et al. (2017) observed that, in human M1, voluntary movement results in supragranular as well as infragranular activation, while somato-sensation leads to activation of the superficial layers of the cortex. At 9,4T in rodents, S.G. Kim observed either glomerular, plexiform or granular activation in response to either odor, electrical stimulation of the lateral olfactory bulb or electrical stimulation of the anterior commissure, respectively (Iordanova et al., 2015). Super-high spatio-temporal resolution fMRI of the barrel cortex employing a line-scanning method at 11.7T demonstrated that somato-sensory stimulation to the whisker or forepaw activates layer 4/5 first, peaking later at layer 2/3 and layer 5 (Yu et al., 2014).

3.3.3. Propagation of spontaneous activity through cortico-cortical connections

In contrast to the evoked studies, resting-state evaluations with cortical depth-specificity have remained scarce, one of the reasons being the difficulty of imaging the whole brain at high resolution. An elegant study in the auditory cortex of rats showed that the propagation pattern of spontaneous activity differs from that observed during sensory-evoked activation, with spontaneous activity following a bottom-up pattern, spreading slowly across columns, and sensory activity initiating in granular layers and reaching neighbor columns at a higher speed (Sakata and Harris, 2009). It is possible that some sub-systems use the same underlying circuit for communication during resting-state and upon stimulation or task performance, e.g., in the visual cortex the columnar behavior during rest resembles the iso-orientation maps obtained during visual stimulation (Vasireddi et al., 2016).

Although the number of resting-state studies with cortical depth-specificity is, at present, insufficient, some reports have shed light on the potential laminar-specific routes supporting resting-state communication. Network specific analysis with high-resolution fMRI in mice suggest that the default mode network (DMN) is especially sustained by supra-granular layers (Whitesell et al., 2021). Whitesell et al., identified voxels associated with the DMN in resting-state scans, and investigated the structural cortico-cortical connectivity affiliated to those voxels. Fibers starting in layer 2/3 mostly targeted other DMN cortical areas, while fibers starting in layer 5 projected to regions external to the DMN. Similarly, resting-state functional connectivity in area 3b and 1 of the monkey, somato-sensory cortex, appeared stronger between superficial and intermediate layers of the cortex (Mishra et al., 2019). In humans, the superficial layers of M1 correlate, at rest, with S1, and both superficial as well as deep layers communicate with the premotor cortex (Huber et al., 2017). Interestingly, activation of the superficial layers but not the deeper layers of mouse motor cortex triggered network-wide events (Weiler et al., 2008). The apparent predominance of the supragranular layers to mediate resting-state connectivity may support the use of microscopy-based techniques to investigate brain networks in rodents.

Despite the multiple efforts to characterize resting state networks within the cortex, to date, no consensus has been reached regarding the cortical depths involved in the presumed connections between hubs. Future studies performed at ultra-high resolution without compromising brain coverage will hopefully shed light on the circuit-specific resting-state fMRI correlation features across cortical layers.

Intracortical connections are one potential source for time-lagged relationships and propagation between cortical areas that are observed with some types of rs-fMRI analysis (Majeed et al., 2011; Mitra et al., 2015; Yousefi and Keilholz, 2021). However, the differences in timing between areas, which are on the order of one second or more, are substantially longer than the time that it takes for synaptic transmission. Another possibility is that the BOLD signal propagation is driven by waves of glial activity. In the hippocampus, there is some evidence that astrocytic calcium waves propagate from cell to cell and are accompanied by changes in infraslow LFPs and blood flow (Kuga et al., 2011).

3.4. Sources of common input and neuromodulation

If areas A and B both receive strong input from area C, A and B can exhibit correlated activity even if there is no direct connection between them. Thus networks of spatially distinct nodes that exhibit correlated activity may contain areas where activity is correlated by direct connections, areas whose correlated activity reflects a common driver, and downstream areas where parallel pathways of input result in correlation despite lack of a direct connection or direct common input. The ability to distinguish between these mechanisms is important for correct interpretation of altered functional connectivity, e.g., in psychiatric disorders.

One challenge in distinguishing possible sources for functional connectivity within a network is that some studies focus only on the cortex, ignoring diencephalon structures that are known to have widespread projections. Animal fMRI studies are less prone to this type of bias, but reports of subcortical involvement in cortical networks are rare, possibly because the subcortical nuclei that project to specific cortical areas are small, comparable to the size of a voxel. Even in stimulus-based studies where subcortical activity is known to occur, it is often undetectable (Keilholz et al., 2004, 2006). It has been, however, possible to detect important subcortical contributions to global cortical responses by using whole brain fMRI in rats; an example being the thalamic involvement in widespread cortical suppression coinciding with spontaneous astrocytic activity (Wang et al., 2018). Another study showed that optogenetic stimulation of the thalamus increased functional connectivity in multiple cortical networks (Wang et al., 2019). Low frequency stimulation of the hippocampus increases interhemispheric functional connectivity, and a chemical blockade of hippocampal activity decreases interhemispheric connectivity (Chan et al., 2017), more evidence of the role that these diencephalon structures play in the coordination of activity across the brain.

3.4.1. Role of neuromodulation in functional connectivity

The size and position of deep brain nuclei makes it difficult to examine their functional connectivity directly. Instead, researchers often pursue a perturbationsl approach. In animal studies, pharmacological, chemogenetic and optogenetic approaches can be used to manipulate signaling from deep brain nuclei. Chemogenetics allows the reversible manipulation of cells upon systemic administration of a drug by targeted expression of specific receptors in their membranes. The most common example of chemogenetics are DREADDS or designer receptors exclusively activated by designer drugs (Campbell and Marchant, 2018). In the case of optogenetics, the putative receptors, also selectively expressed in particular cell populations, are sensitive to light pulses delivered by optical fibers, the most common being Ch R2 (Boyden et al., 2005). Both techniques, together with common pharmacological approaches, constitute an essential tool to interfere with the nervous system and study network vulnerability or modulation. A substantial body of literature has shown that manipulation of catecholamine systems results in altered functional connectivity, both in humans and in animals (Shah et al., 2015; Shah et al., 2016).

Over the years, a number of neuromodulatory nuclei and neurotransmitter systems have been proposed as candidates to drive common input via neuromodulation of cortical networks, including but not limited to the rostral ventrolateral medulla (Golanov and Reis 1996; Drew et al., 2008), the basal forebrain (Nair et al., 2018; Turchi et al., 2018) and cholinergic system, the raphe nucleus (Razoux et al., 2013; Shah et al., 2016) and serotonin, ventral tegmental area and dopamine (Decot et al., 2017), and locus coeruleus and norepinephrine (Zerbi et al., 2019). Neuromodulatory systems are often thought of as having widespread and diffuse projections, which would make them an unlikely source of common input for the spatially structured functional networks that are observed with rs-fMRI. However, there is a growing appreciation for the diversity of spatial and temporal structure that these nuclei can provide (van den Brink et al., 2019; Coletta et al., 2020). Differences in the receptor type and/or receptor density across brain areas ensures that the same input can have regionally distinct effects (Lindvall et al., 1978; Atzori et al., 2016; Kim et al., 2016; Disney and Higley, 2020; Sarter and Lustig, 2020), even at the laminar level (Palomero-Gallagher and Zilles, 2019). Moreover, there is growing evidence that neuromodulatory nuclei themselves are heterogenous, with different populations of cells exhibiting different patterns of input or types of activity (Li et al., 2018; Totah et al., 2018; Zaborszky et al., 2018; Disney and Higley, 2020; Sarter and Lustig, 2020).

One way in which neuromodulatory nuclei might act is to alter the response to incoming stimuli. For example, by reducing intrinsic fluctuations of activity, the signal-to-noise ratio of activity related to sensory input could be improved. Lottem et al., (Lottem et al. 2016) have shown that serotonin can act in this way, quenching spontaneous fluctuations while sparing sensory-evoked activity. This is consistent with work by Grandjean et al. (2019), showing that optogenetic stimulation of the dorsal raphe nuclei reduced blood volume and neural activity across wide areas of the cortex. Other neurotransmitters act in a similar manner; activation of the cholinergic system also reduces spontaneous activity while leaving evoked activity unaffected (Meir et al., 2018). In contrast, a recent study showed that chemogenetic activation of the locus coeruleus increased functional connectivity throughout much of the cortex (Zerbi et al., 2019).

It is probably overly simplistic to think of spatial correlations as arising from a single neuromodulatory system. Deep brain nuclei are interconnected and their interactions may be complex. For example, dopamine has a well-characterized role in cortico-striatal and mesolimbic theta oscillations, but norepinephrine levels also play a behaviorally-relevant role in coordination across these areas (Dzirasa et al., 2010). In another case, norepinephrine drives activity in midline thalamic areas through a dopaminergic mechanism (Beas et al., 2018). In humans, a rs-fMRI study found that dopaminergic areas in the midbrain and the serotonergic dorsal raphe nuclei were part of the default mode network, while the locus coeruleus and the remaining serotonergic nuclei were integrated with the executive control network (Bar et al., 2016). This suggests that neuromodulatory nuclei could together account for the general functional organization of the brain into two anticorrelated networks.

Neuromodulatory nuclei are known to alter cerebral perfusion. Stimulation of the basal forebrain and locus coeruleus both induce vasodilation, which may be mediated partly by interneurons and depend on the state of the brain (Kocharyan et al., 2008; Lecrux and Hamel, 2016), offering another method for localized differences in the response to neuromodulatory input. Because components of the neurovascular unit have receptors for neurotransmitters (e.g., norepinephrine), a local increase in neuromodulator could potentially modify neurovascular coupling and affect the fidelity of the hemodynamic response to a given neuronal activation (Lecrux et al., 2017). Thus another contribution to functional connectivity could arise from neurotransmitter-mediated changes in the "signal-to-noise" of the rs-fMRI signal, in terms of its sensitivity to neural activity. While the amplitude of two signals does not affect the correlation between them, an increase in the noise level results in lower correlation, which would appear as a reduction of functional connectivity.

3.4.2. Arousal levels and functional connectivity

Dynamic analysis might provide more insight into how neuromodulation contributes to functional connectivity. For example, arousal levels are primarily driven by the ascending reticular activating system (ARAS), which arises in the brainstem and then innervates the cortex directly or via the thalamus. It is usually considered to include neurotransmitter-specific pathways from the locus coeruleus, raphe nuclei, and ventral tegmental area, among others. Arousal levels are known to vary over the course of the typical rs-fMRI scan, even in subjects attempting to remain awake. Several studies that look at brain states over the course of a rs-fMRI scan have identified particular states that ap-

pear to be associated with drowsiness, as they become more frequent as the scan progresses and occur in conjunction with other features of reduced alertness (Chang et al., 2013a, 2013b; Allen et al., 2014; Tagliazucchi and Laufs, 2014; Chang et al., 2016; Falahpour et al., 2018). The strong contribution of arousal to dynamic functional connectivity ensures that it also plays a role in time-averaged functional connectivity, and suggests that fluctuations in neuromodulatory input related to other neurophysiological processes can influence the spatial structure of the BOLD fluctuations. In fact, the strength of connections between hubs in the human DMN is strongly correlated with the integrity of the arousal system of the brain, e.g. patients suffering from severe disorders of consciousness exhibit weaker connections (Vanhaudenhuyse et al., 2010). Similarly, a rat model of brainstem coma showed increased functional connectivity as animals regained arousal (Pais-Roldan et al., 2019).

Templates of brain activity related to alertness level have been identified for both humans and monkeys (Chang et al., 2016; Falahpour et al., 2018). To date, no such template exists for rodents, partly because the vast majority of rodent studies are conducted under anesthesia. There is evidence that the repertoire of brain states is reduced by anesthesia in the rodent (Hudetz et al., 2015). However, substantial variability is observed in brain states based on sliding window correlation or coactivation patterns in anesthetized rodents (Keilholz et al., 2013; Zhang et al., 2020), an indication that fluctuations in arousal level may occur, at least to an extent, under anesthesia. Interestingly, arousal fluctuations tracked as varying pupil dynamics in anesthetized rats were accompanied by correlated rs-fMRI maps (Pais-Roldan et al., 2020). The fact that the brain state fluctuates at the within-subject short-term level indicates that network patterns of rs-fMRI are necessarily complex and subjected to external modulation.

3.4.3. Neuromodulation and repeated spatiotemporal patterns of activity

Neuromodulatory input might also account for some of the repeated spatiotemporal patterns of activity that are observed in rs-fMRI (Majeed et al., 2009; Majeed et al., 2011; Thompson et al., 2014; Belloy et al., 2018; Yousefi et al., 2018; Abbas et al., 2019; Belloy et al., 2021) (quasiperiodic patterns or QPPs). These patterns, which are remarkably consistent across individuals, involve propagation along the cortex and account for a large portion of the functional connectivity that is observed in humans (Yousefi and Keilholz, 2021). Similar patterns have been observed in both neural activity and hemodynamics in mice using optical imaging, and as in humans, the phase of the propagating wave appears to dictate the coactivation patterns of cortical areas (Matsui et al., 2016). The repetitive nature of the patterns and the stereotyped timing of activation and deactivation implies that they are a fundamental feature of the brain's intrinsic organization, rather than a response to external stimuli or internal processing, and direct white matter connections alone are not sufficient to account for the fairly complex patterns of signal propagation that are observed (Kashyap and Keilholz, 2019). In rodents, the patterns include deactivation in the reticular formation accompanied by widespread cortical activation (Belloy et al., 2021). This finding is the inverse of prior work showing cortical deactivation when neuromodulatory nuclei were stimulated. In humans, areas in the brainstem and thalamus lead the changes in cortical activation, which suggests the mechanisms that drive QPPs are similar across species (Yousefi and Keilholz, 2021).

In support of a neuromodulatory source for QPPs, QPPs were found to contribute less to functional connectivity in patients with attention deficit hyperactivity disorder (ADHD) than healthy controls, consistent with a reduction in neuromodulatory input (Abbas et al., 2019). In rats, the patterns appear to reflect infraslow electrical activity (Pan et al., 2013; Thompson et al., 2014), and the timing varies from a cycle of ~5–6 s in animals sedated with dexmedetomidine to 10 + seconds in animals under isoflurane anesthesia (Thompson et al., 2014), again consistent with the differing levels of arousal. Moreover, alterations in these patterns were observed in a mouse model of Alzheimer's, as expected given the early degeneration of neuromodulatory nuclei in this disorder (Belloy et al., 2018).

It is worth noting that both widespread patterns of neural activity (e.g., QPPs) and the global signal (as described in a later section) may be linked to neuromodulation. In some ways, this is not surprising, since high global signal amplitudes necessarily reflect widespread patterns of strong, coherent activity. However, the question remains of whether the global average signal contains additional information about arousal and neuromodulation that is independent of the contribution from large-scale spatial patterns.

Given the variety of ways that neuromodulatory input from deep brain nuclei can potentially coordinate neural activity, more experiments that capture the BOLD signal along with the local changes in neuromodulator concentration using sensor imaging are badly needed (Sabatini and Tian, 2020). Techniques that can capture the effects of neuromodulators throughout the whole brain, rather than in single areas, will be particularly valuable in unraveling the role that these deep brain nuclei play in organizing large scale brain activity.

3.4.4. Other sources of common input

Other potential sources of common input include autonomic processes like respiration and cardiac pulsation. Both can introduce spatially distributed, correlated noise that overlies the fluctuations related to neural activity, and while in principle this noise can be removed using a number of approaches, in practice this is difficult because both processes also are maintained by active networks in the brain. The primary respiratory centers, for example, are in the medulla and pons, but respiration is also under voluntary control regulated by the cortex, and it is well known that both heart rate and respiration patterns change with the subject's overall state (for example, breathing and heart rate slow as a person falls asleep). As one example of the interconnectedness of arousal and autonomic functions, heart rate variability covaries with functional connectivity in networks associated with arousal (Chang et al., 2013). Moreover, global BOLD fluctuations vary with vascular tone in the extremities, which has suggested that sympathetic innervation of the vasculature in the brain may impact rs-fMRI. The photoplethysmography (PPG) signal from the finger typically drops following EEG K complexes, along with the global fMRI signal (Ozbay et al., 2018), suggesting that intermittent sympathetic activation changes the rs-fMRI signal.

Many studies in humans have drawn attention to the effect of respiration and cardiac cycles on resting state networks (Birn et al., 2006; Chang et al., 2009; Chen et al., 2020). In typical animal experiments, the difference in field strength, relative geometry of the coil and chest cavity, and differences in respiratory and cardiac rates could cause the "noise" component from these cycles to be quite different than in humans. In particular, the faster physiological rates in rodents, not accompanied by proportionally faster fMRI acquisition rates, usually lead to signal aliasing (Pais-Roldan et al., 2018).

Often forgotten as potential sources of coordinated brain activity are other rhythmic interoceptive inputs. For example, the gut and brain interact continuously, and the digestive system produces rhythmic pulses that could influence spontaneous activity in the brain. Cao et al. (2019) showed that stimulation of the stomach resulted in widespread activation in sensory and cingulate cortices. The general tendency to treat the brain as an isolated system may need to be abandoned if we hope to fully understand how spontaneous activity is structured (Stringer et al., 2019).

3.4.5. The vasculature as source of a common signal

Another easily-overlooked source of a common signal across widespread brain areas is the vasculature. The hemodynamic response to spontaneous activity is much the same as the response for evoked activity, but other oscillations that are effectively removed by averaging during stimulus-based studies could contribute to widespread coherent fluctuations in the BOLD signal. Vasomotor oscillations are present in arterioles even when they are isolated from neural input (Osol and

Halpern, 1988) and slow arteriole dilations are conserved in the absence of neuronal activity (Winder et al., 2017). Spontaneous neuronal activity precedes and can entrain low-frequency vascular oscillations (Mateo et al., 2017; Gu et al., 2018). Because vasomotion is affected by changes in blood pressure (Koenigsberger et al., 2006), systemic blood pressure changes could modulate the apparent connectivity within networks by increasing or reducing the signal to noise ratio of the BOLD fluctuations. Indeed, the low frequency BOLD oscillations increase in amplitude when blood pressure decreases (Kannurpatti et al., 2008). The amplitude and frequency of vasomotor oscillations depend on vascular features such as vessel diameter and wall thickness (Koenigsberger et al., 2006) and could contribute to parcellations in the frequency of vasomotion observed in fMRI experiments (Mitra et al., 1997).

One of the appealing aspects of vasomotion as the temporal signature of functional connectivity is the relatively symmetrical nature of the vasculature across the midline. If the vasomotor oscillations are also symmetric, that might account for the very strong interhemispheric BOLD correlations that remain when the primary spatiotemporal patterns are removed by regression, and which also appear in areas that are not strongly connected across hemispheres (Yousefi and Keilholz, 2021). An intriguing study by Bauer et al., found that optogenetic stimulation of excitatory neurons from different cortical areas resulted in patterns of activity that were less bilaterally symmetric than the hemodynamic-based functional connectivity from the same areas (Baek et al., 2016). Another study found that the brain of the zebra finch, which lacks a corpus callosum, exhibited strong bilateral functional connectivity (Kundu et al., 2014). It is possible that the vasomotor oscillations amplify oscillations of neural activity, or, since interstitial oxygen and ionic concentrations might be actively modulated by the vascular oscillations, they might even influence local neuronal activity via slow potential modulation.

3.5. Global signal

The global signal referred to in fMRI is defined as an average time course across all voxels of the cortex or all of the brain. Although a certain correlation with this average time course can be observed globally, the signal has been shown to reflect the activity of certain networks (Fox et al., 2009). The global signal is often removed during fMRI preprocessing because it also contains contributions from physiological noise; however, this almost certainly removes some neuronal signal as well. While a large portion of the global signal comes from non-neuronal contributors, e.g., thermal noise, cardiac or respiratory function, motion, hardware artifacts, etc. (Murphy et al., 2013; Power et al., 2017a, 2017b; Drew et al., 2020), several studies have also demonstrated a neurobiological source. For instance, in monkeys, the global fMRI signal correlates with electrophysiological recordings (Scholvinck et al., 2010), in mice, the phase of the global signal determines hemodynamic and calcium-based neuronal coactivation in the neocortex (Matsui et al., 2016) and brain-state fluctuations assessed with external arousal indicators (e.g., eye blinks or pupil size) have demonstrated a strong correlation with the global functional dynamics in monkeys and rats (Chang et al., 2016; Pais-Roldan et al., 2020). Interestingly, the global signal appears to be modulated by the activity of the basal forebrain, as its amplitude decreases upon inactivation of the nucleus basilis of meynert specifically within the altered hemisphere (Musch and Honey, 2018; Turchi et al., 2018). Recent studies suggest a relationship between the global signal and the sympathetic tone, as well as with fluctuations in subcortical arousal, as observed during sleep in animals and humans (Fukunaga et al., 2006; Liu et al., 2015; Ozbay et al., 2019). The dependence of the global signal on the autonomic system is supported by the fact that autonomically-triggered vasodilation leads to higher fMRI signal (Wise et al., 2004; de la Cruz et al., 2017) and that skin vascular tone, also correlated with the global signal, is regulated by the sympathetic nervous system (van Houdt et al., 2010; Tong et al., 2013; Ozbay et al., 2018; Shokri-Kojori et al., 2018).

Unlike in human studies, where the global signal contains major contributions from motion and physiological noise, the global signal in typical experiments on rodents exhibits less contamination from these processes. The majority of rodents are anesthetized and restrained in a stereotaxic head holder for rs-fMRI, which greatly reduces motion. In some studies, rodents are also given a paralytic and mechanically ventilated, which further reduces motion and ensures that contributions from respiratory variation are minimal. Despite these stringent controls, global signal excursions that involve both cortical and subcortical areas can be identified (Fig. 5). Further studies on the neural basis of global signal modulations should leverage the well-controlled conditions in the rodent to maximize sensitivity to the underlying processes.

Besides noise and neuronal activity, the CSF dynamics may also contribute to the global signal, as suggested by the coupling observed between the flow of CSF into the brain (4th ventricle) and slow-wave sleep (Fultz et al., 2019). Interestingly, despite a reduction of cerebral blood flow and metabolism of oxygen and glucose, the global BOLD fMRI signal increases during non-REM sleep (McAvoy et al., 2019). Given the strong evidence supporting a certain neurobiological significance of the global signal, its removal in resting-state studies must be justified and taken into consideration during interpretation of resting-state results (Fox et al., 2009).

The variety of mechanisms that might mediate the organization of activity across the brain should make it clear that it is unlikely that any single one of them fully accounts for the complex spatial structure and temporal dynamics that are observed. Instead, we believe that the concerted effects of multiple processes contribute to functional connectivity, and that different processes might become the dominant contributors under different conditions (see Fig. 6 for one possible model). In this scenario, differences that arise in patient populations may represent a change in the dominant source of coordination, rather than a change in the underlying network structure.

4. Future directions

4.1. The need for technology development

The field of human fMRI has advanced substantially over the last decade, with developments in hardware and software supporting image acquisition at higher spatial and temporal resolution (e.g., following Human Connectome Project protocols Van Essen et al. 2013). These have led to standardized imaging protocols that are widely adopted and which facilitate public data sharing and reanalysis.

In animal rs-fMRI, less progress has been made. Acquisition methods and analysis tools that are routinely used in humans are still not widely available for rs-fMRI studies in animals. The combination of the high field strengths and small size of the rodent brain makes it difficult to design coils suitable for high acceleration factors, and without the potential of clinical adoption, it is difficult to fund the needed development of hardware and software. Moreover, only the most recently-upgraded animal scanners have multichannel capabilities. However, most preclinical MRI systems operate at higher field strengths (7T +) than human scanners, have stronger gradients, and impose less stringent limitations on SAR and gradient switching. There is a need to leverage these advantages along with new technology from human scanners to create an approach that is specifically tailored to neuroimaging of the rodent brain.

One exciting recent development is the use of zero-TE sequences like multiband SWIFT for functional imaging in rodents (Lehto et al., 2017; Paasonen et al., 2020). With the high magnetic fields of preclinical MRI systems and the close proximity of the rodent brain to susceptibility gradients, particularly in the ear canals, distortion and signal loss are major challenges. Zero-TE sequences minimize these effects, and even more, are robust to susceptibility artifacts caused by implanted electrodes or optical fibers for multi-modal experiments. The challenge is that the source of functional contrast for these sequences remains poorly un-

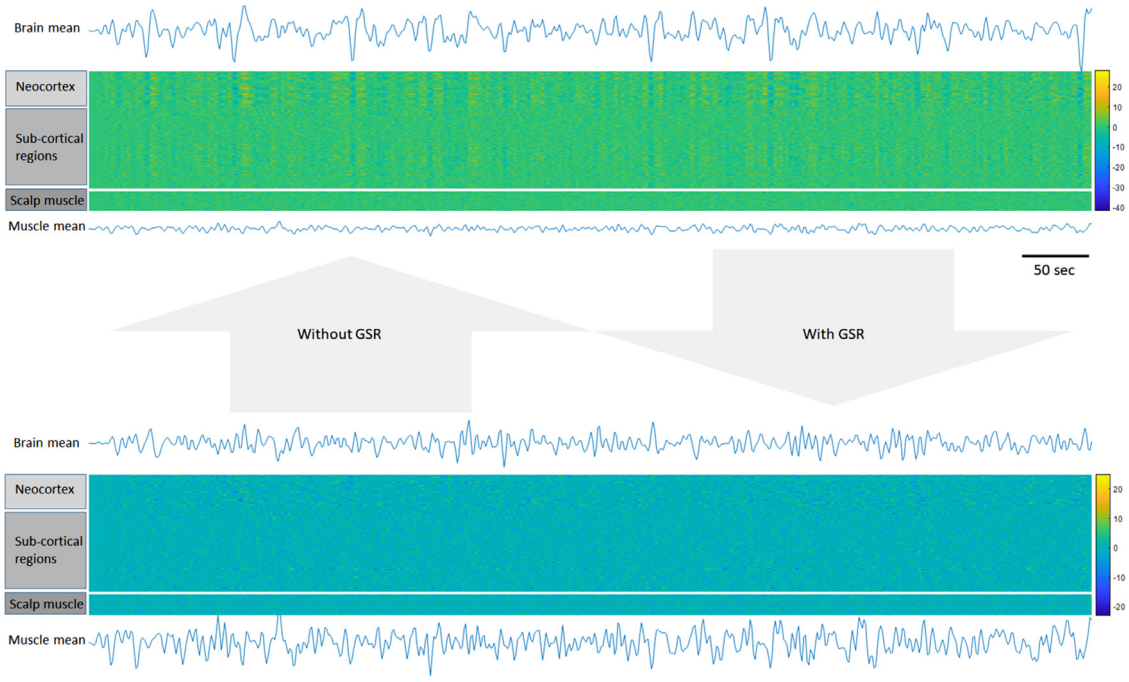

Fig. 5. *Significant global signal modulation not linked to noise*. In a typical rodent fMRI study, head motion and breathing variability is minimized by the use of anesthesia and artificial ventilation in paralyzed animals. For example, under a mixture of dexmedetomidine and low-dose isoflurane, synchronized patterns can be identified visually in both neocortex and subcortical regions (top), but are not reflected in the neighboring scalp tissue, which exhibits relatively small amplitude changes over time despite having comparable baseline signal intensity. The global signals are unlikely to be created by head motion or physiological variation given the stringent restraints and paralytic agents employed. Thus rodent models may offer a unique platform for the investigation of global neural modulation, relatively free from contamination from physiological noise. The global modulation can also be removed by global signal regression (GSR), shown in the bottom panel.

derstood, making translation to humans less straightforward. Still, the animal models provide the ideal opportunity for identifying the source of functional contrast, which may reflect the same underlying processes as the BOLD signal.

Zero-TE sequences could prove to be the key to unlocking another challenge of rs-fMRI in rodents: the use of anesthesia. The vast majority of rodent studies are still performed under anesthesia, with isoflurane and/or dexmedetomidine popular choices. Anesthesia is considered essential for minimizing motion and stress in untrained animals, but also results in a potential confound for translating results to rs-fMRI in awake humans. Many researchers have attempted to move rs-fMRI experiments to awake animals, some with relative success (Peeters et al., 2001; King et al., 2005; Brydges et al., 2013; Reed et al., 2013; Changi et al., 2016; Stenroos et al., 2018; Han et al., 2019) but the approach remains challenging and not widely used. For awake studies, animals are typically accustomed to restraint and the noise of the scanner over the course of several days. Low noise sequences like multi-band (MB) SWIFT might reduce the stress imposed by the scanner environment and improve the quality of studies in awake animals. Moreover, MB-SWIFT is relatively insensitive to the body motion of the animal in the scanner (Paasonen et al., 2020), unlike EPI-based sequences where even respiratory motion can introduce substantial artifacts (Raj et al., 2000; Kalthoff et al., 2011). MB-SWIFT could therefore allow quiet scans while relaxing the strenuous constraints on animal movement, a major step forward for awake animal studies.

Meanwhile, the use of anesthesia to minimize stress and motion is likely to continue to predominate in rodent fMRI studies (Becq et al., 2020). Recent investigations have been exploring a compromise approach that minimizes the dosage of anesthetic and the resulting vascular effects. For example, a mixture of dexmedetomidine and a low dose of isoflurane appears capable of creating a stable brain state of light anesthesia that can extend for hours (Brynildsen et al., 2017), providing flexibility in the experimental approach to acquire more scans from each animal under conditions that are comparable across designs and different subjects.

In terms of analysis, preprocessing pipelines and noise removal are not as well-developed for rodents as for humans (Chuang et al., 2019). Motion, cardiac and respiratory signals of animals and humans interfere with the fMRI time courses, especially in the brain edges, brainstem and areas near the main blood vessels of the brain (Teichert et al., 2010; Birn et al., 2014; Griffanti et al., 2017; Keilholz et al., 2017; Sclocco et al., 2018; Yoshikawa et al., 2020). Although the physiological noise is similarly distributed in animals and humans, its distinct temporal features make the identification of physiological noise more complex in rodent fMRI; the respiratory and cardiac cycle in rodents happens at rates approximately five times faster than in humans (Williams et al., 2010; Fleming et al., 2011; Pais-Roldan et al., 2018), which translates into a poorer sampling of these signals with fMRI and consequently more difficult removal from the data. One approach to denoise animal fMRI data is to modify human preprocessing protocols, e.g., training a FIX classifier (Salimi-Khorshidi et al., 2014) for mice (Zerbi et al., 2015). As in human studies, multi-echo sequences have been used to determine which components of the MRI signal do not exhibit BOLD-like $T2^*$ dependence and are therefore likely to be noise (Kundu et al., 2014), although this comes at the expense of slower sampling rates and more complex analysis.

The rodent neuroimaging community has begun to work towards the goal of improved standardization and data sharing by examining rs-fMRI data from mice acquired across multiple institutions (Mandino et al., 2019). The time is ripe to create a hub for rodent neuroimaging data, which would encourage exploratory analysis, allow comparisons between different protocols from different labs, make reproducibility analyses feasible, and facilitate collaborations (Mandino et al., 2019). Such a database would be highly complementary to the Allen brain atlas, which provides a wealth of information about gene expression and tracer injections that provide valuable context for functional neuroimaging studies.

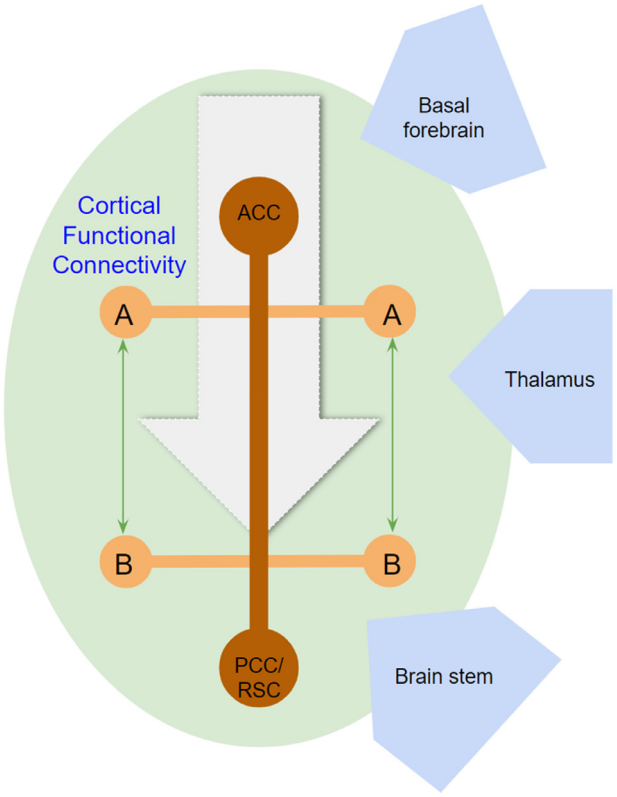

Fig. 6. An illustrative model of how different neurophysiological processes might act in concert to produce patterns of coordinated activity. Direct white matter connections, for example along the midline between the anterior cingulate and the retrosplenial cortex and between homologous areas in the left and right hemisphere, form a framework for 'fast-pass' interactions and synchronized oscillations. Less direct connections, for example intracortical connections within each hemisphere, could modify the phase or amplitude of activity in other areas. Common projections from the basal forebrain might drive waves of propagating activity from anterior to posterior areas (Massimini et al., 2004); input from the locus coeruleus and thalamus (Neske, 2015) might modulate the overall level of excitation and slow cortical oscillations. The resulting patterns of activity are filtered through the overlying vascular structure, which may enhance the interhemispheric symmetry.

Databases for transgenic animals and disease models could be particularly valuable to the community.

4.1.1. Linking whole brain activation to neural circuits

Neuroscience as a field has traditionally had a heavy focus on circuit-level descriptions of brain activity, many of which have been studied in rodent models using invasive techniques that can identify individual cells or even individual synapses. Functional MRI studies in rodents have begun to bridge the gap between these careful circuit characterizations and the systems level activity of the brain.

Whole brain rs-fMRI is typically used to detect interconnected hubs. Although a series of (mostly cortical) networks have been identified in the human and animal brain, the specific groups of neurons that are recruited for each of those networks (e.g., granule cells, pyramidal cells, etc.) remains to be deciphered. To specifically define the circuit underlying functional connectivity between two remote areas, a required step would be to detect the cortical layers in both territories that exhibit a high temporal correlation. This additional dimension, i.e. the cortical depth in a layer-specific resting-state connectivity analysis, could bring into play new features to characterize the brain function.

Beyond the mesoscale, besides specific cortical layers and cell types, the synapse type between cortical areas may modulate, at some extent, the behavior of brain networks (Covic and Sherman, 2011). Emerging studies combining fMRI with calcium imaging, optogenetics and novel stimulation methods like focal infrared neural stimulation may enable the community to dissect, with unprecedented detail, cortical networks as well as the underlying vascular networks in animal models (Chernov and Roe, 2014; Albers et al., 2018; He et al., 2018; Wang et al., 2018; Chenn et al., 2019; Xu et al., 2019).

4.1.2. Linking brains and behavior

Most broadly, neuroscience aims to link patterns of brain activity to behavior. Functional connectivity has much promise in this regard, with recent studies showing, for example, associations between network structure and changes in attentional states (Kucyi et al., 2020; Rosenberg et al., 2020), working memory (Yamashita et al., 2018; Avery et al., 2020), and many other behavioral and psychological phenomena (Woodward and Cascio, 2015; Li, Hu et al., 2019; Yan et al., 2019). A key challenge is to distinguish causal from non-causal relationships (Pearl, 2009). Here animal models will be crucial. The interventional experiments necessary to show that specific patterns of connectivity drive particular behaviors cannot be conducted within humans. Behavioral interventions – inducing a change in behavior and then observing a corresponding change in connectivity-cannot establish causality. Physiological interventions are necessary, but those available in humans are not specific enough nor powerful enough for the task at hand. While we cannot yet define exactly what the required experiments will look like, it is clear that they will have to be conducted in animal models.

4.1.3. Signatures of specific types of activity or neurophysiological processes

Given that the BOLD signal is an integrative representation of a wide variety of neurophysiological processes, possibly with additional contributions from the vasculature, and that it is inevitably contaminated with a variety of noise, it is daunting to contemplate the challenge of interpreting functional connectivity, especially when it comes to alterations observed in patients with psychiatric or neurological disorders. Attempting to localize a single cause for a change in functional connectivity might be analogous to trying to listen to a single flute player in a poorly-recorded orchestra. Nevertheless, there are clues that might help to determine which factor dominates in a particular situation.

It is important to use all of the tools at our disposal. To obtain the fullest picture of how the BOLD fluctuations are organized, we must move beyond time-averaged functional connectivity and consider temporal and spectral information as well. As an example, spatial patterns that recur periodically over time are unlikely to reflect transient sensory stimuli or cognitive processes, while short periods of high activity in sensory and motor areas could be related to body motion. The power spectrum of the BOLD signals may help to isolate periodic contributors, whether well-known like respiration and cardiac pulsation, or more obscure, like gastric oscillations. The spatial specificity of changes may imply a source: downstream effects of a change in neuromodulatory input would be expected to be widespread, while effects of a change in connectivity between two areas of interest should be more localized. Spatial specificity might be especially useful in high resolution studies that can resolve laminar activity, since much is known about the distribution of input and output connections in particular layers of some cortical areas.

Similarly, the explosion of machine learning has popularized efforts to learn something about the underlying neural activity from the BOLD fluctuations, but the exercise remains speculative in nature unless there is a way to validate the output. For example, using a recurrent neural network (RNN), one can learn the coefficients of the Wilson-Cowan model to parse firing rates or excitatory and inhibitory currents from the BOLD data (Kashyap and Keilholz, 2020). By forcing the RNN to output interpretable parameters, the way is paved for the multimodal experiments that are essential for the ultimate validation.

In all cases, findings from rs-fMRI need to be placed in the context of more specific information obtained with other modalities. With the

help of these tools, the interpretation of functional connectivity remains challenging but perhaps not hopeless.

4.1.4. Testing models of the brain

Animal models have always provided a platform where models of brain activity could be tested using targeted but invasive methods such as physical or chemical lesioning, electrical stimulation, or pharmacological manipulations. New advances in selective manipulations using optogenetic stimulation or DREADDs provide an unprecedented degree of selectivity and control, opening new possibilities for understanding how different types of neural or glial cells contribute to the hemodynamic response, or how particular areas are involved in the coordination of activity across the brain (Ryali et al., 2016). At the same time, new imaging and recording developments, many of which were supported by the BRAIN initiative, have made it possible to study the coordination of neural activity across the brain in ways that were not possible before. These studies, in combination with rs-fMRI, allow us to build new and better models of how the brain works.

The ultimate test of any model is how well it predicts what will happen when some component of the model is perturbed. For example, one could build a brain network model based on a particular neural mass model at each node and prameterized to fit rs-fMRI data, then predict what happens when the activity at a specific node is increased. To test the prediction, one might acquire rs-fMRI data during optogenetic stimulation of the same node, and compare the experimental results to those predicted by the model. The process sounds simpler than it is, given the technical constraints of optogenetic stimulation and the challenges of reproducing the effects of stimulation with a particular neural mass model, but the framework is valid and offers a powerful way to advance our understanding of how the brain works by leveraging interventions available in animal models.

5. Conclusions

Coordination of activity across distant areas of the brain as measured with functional connectivity has proven to be necessary for normal function, e.g., disruptions in connectivity are often associated with neurological or psychiatric disorders. However, functional connectivity has not been adopted as a clinical tool for routine diagnosis and evaluation, possibly because the source and role of these coupled oscillations remains poorly characterized. A better understanding of the specific processes that contribute to BOLD fluctuations and functional connectivity could move rs-fMRI beyond a biomarker to an informative tool for the diagnosis or evaluation of brain disorders. While data from human subjects provides insight into the implications of functional connectivity for cognitive processes, animal studies are crucial to understand the underlying neurophysiology. At the same time, these studies will improve understanding of the systems-level organization of the brain, bridging between more localized studies of neural circuits and the macroscopic functional architecture of the brain. The identification of particular neurophysiological processes that are reflected in the BOLD fluctuations could improve sensitivity to changes related to cognition and behavior, and provide a more mechanistic explanation of the processes involved.

Data and code

As this is a review paper, no new data or code are presented.

Credit authorship contribution statement

Patricia Pais-Roldán: Visualization, Writing – review & editing. **Celine Mateo:** Visualization, Writing – review & editing. **Wen-Ju Pan:** Visualization, Writing – review & editing. **Ben Acland:** Visualization, Writing – review & editing. **David Kleinfeld:** Visualization, Writing – review & editing. **Lawrence H. Snyder:** Visualization, Writing – review & editing. **Xin Yu:** Visualization, Writing – review & editing. **Shella Keilholz:** Visualization, Writing – review & editing.

Funding information/Acknowledgements

SK and W-J P: R01MH111416, R01NS078095, R01EB029857, R01AG062581, NSF 1822606, 1533260; XY: RF1NS113278, R01NS122904; LHS+BA: R34NS118618, R01EY012135; DK R35NS097265, R01MH111438 (includes CM, XY). The authors would like to thank Prof. Jochen Staiger for helpful discussions.

References

Abbas, A., Bassil, Y., Keilholz, S., 2019. Quasi-periodic patterns of brain activity in individuals with attention-deficit/hyperactivity disorder. Neuroimage Clin. 21, 101653.
Abbas, A., Belloy, M., Kashyap, A., Billings, J., Nezafati, M., Schumacher, E.H., Keilholz, S., 2019. Quasi-periodic patterns contribute to functional connectivity in the brain. Neuroimage 191, 193–204.
Adams, D.L., Piserchia, V., Economides, J.R., Horton, J.C., 2015. Vascular Supply of the Cerebral Cortex is Specialized for Cell Layers but Not Columns. Cereb. Cortex 25 (10), 3673–3681.
Adelsberger, H., Garaschuk, O., Konnerth, A., 2005. Cortical calcium waves in resting newborn mice. Nat. Neurosci. 8 (8), 988–990.
Ahrens, K.F., Levine, H., Suhl, H., Kleinfeld, D., 2002. Spectral mixing of rhythmic neuronal signals in sensory cortex. Proc. Natl. Acad. Sci. U. S. A. 99 (23), 15176–15181.
Albers, F., Wachsmuth, L., van Alst, T.M., Faber, C., 2018. Multimodal functional neuroimaging by simultaneous BOLD fMRI and fiber-optic calcium recordings and optogenetic control. Mol. Imaging Biol. 20 (2), 171–182.
Allaway, K.C., Munoz, W., Tremblay, R., Sherer, M., Herron, J., Rudy, B., Machold, R., Fishell, G., 2020. Cellular birthdate predicts laminar and regional cholinergic projection topography in the forebrain. Elife 9, e63249. doi:10.7554/eLife.63249.
Allen, E.A., Damaraju, E., Plis, S.M., Erhardt, E.B., Eichele, T., Calhoun, V.D., 2014. Tracking whole-brain connectivity dynamics in the resting state. Cereb. Cortex 24 (3), 663–676.
Anenberg, E., Chan, A.W., Xie, Y., LeDue, J.M., Murphy, T.H., 2015. Optogenetic stimulation of GABA neurons can decrease local neuronal activity while increasing cortical blood flow. J. Cereb. Blood Flow Metab. 35 (10), 1579–1586.
Atasoy, S., Donnelly, I., Pearson, J., 2016. Human brain networks function in connectome-specific harmonic waves. Nat. Commun. 7, 10340.
Attwell, D., Mishra, A., Hall, C.N., O'Farrell, F.M., Dalkara, T., 2016. What is a pericyte? J. Cereb. Blood Flow Metab. 36 (2), 451–455.
Atzori, M., Cuevas-Olguin, R., Esquivel-Rendon, E., Garcia-Oscos, F., Salgado-Delgado, R.C., Saderi, N., Miranda-Morales, M., Trevino, M., Pineda, J.C., Salgado, H., 2016. Locus ceruleus norepinephrine release: a central regulator of CNS spatio-temporal activation? Front. Synaptic Neurosci. 8, 25.
Avery, E.W., Yoo, K., Rosenberg, M.D., Greene, A.S., Gao, S., Na, D.L., Scheinost, D., Constable, T.R., Chun, M.M., 2020. Distributed patterns of functional connectivity predict working memory performance in novel healthy and memory-impaired individuals. J. Cogn. Neurosci. 32 (2), 241–255.
Baek, K., Shim, W.H., Jeong, J., Radhakrishnan, H., Rosen, B.R., Boas, D., Franceschini, M., Biswal, B.B., Kim, Y.R., 2016. Layer-specific interhemispheric functional connectivity in the somatosensory cortex of rats: resting state electrophysiology and fMRI studies. Brain Struct Funct 221 (5), 2801–2815.
Baillarger, 1840. Recherches sur la structure de la couche corticale des circonvolutions du cerveau. Mém. Acad. R. Méd. 8 149–83.
Bandettini, P.A., Wong, E.C., Hinks, R.S., Tikofsky, R.S., Hyde, J.S., 1992. Time course EPI of human brain function during task activation. Magn. Reson. Med. 25 (2), 390–397.
Bar, K.J., de la Cruz, F., Schumann, A., Koehler, S., Sauer, H., Critchley, H., Wagner, G., 2016. Functional connectivity and network analysis of midbrain and brainstem nuclei. Neuroimage 134, 53–63.
Barks, S.K., Parr, L.A., Rilling, J.K., 2015. The default mode network in chimpanzees (Pan troglodytes) is similar to that of humans. Cereb. Cortex 25 (2), 538–544.
Beas, B.S., Wright, B.J., Skirzewski, M., Leng, Y., Hyun, J.H., Koita, O., Ringelberg, N., Kwon, H.B., Buonanno, A., Penzo, M.A., 2018. The locus coeruleus drives disinhibition in the midline thalamus via a dopaminergic mechanism. Nat. Neurosci. 21 (7), 963–973.
Becq, G.J.C., Barbier, E.L., Achard, S., 2020. Brain networks of rats under anesthesia using resting-state fMRI: comparison with dead rats, random noise and generative models of networks. J. Neural Eng. 17 (4), 045012.
Belcher, A.M., Yen, C.C., Stepp, H., Gu, H., Lu, H., Yang, Y., Silva, A.C., Stein, E.A., 2013. Large-scale brain networks in the awake, truly resting marmoset monkey. J. Neurosci. 33 (42), 16796–16804.
Belloy, M.E., Billings, J., Abbas, A., Kashyap, A., Pan, W.J., Hinz, R., Vanreusel, V., Van Audekerke, J., Van der Linden, A., Keilholz, S.D., Verhoye, M., Keliris, G.A., 2021. Resting brain fluctuations are intrinsically coupled to visual response dynamics. Cereb. Cortex 31 (3), 1511–1522.
Belloy, M.E., Naeyaert, M., Abbas, A., Shah, D., Vanreusel, V., van Audekerke, J., Keilholz, S.D., Keliris, G.A., Van der Linden, A., Verhoye, M., 2018. Dynamic resting state fMRI analysis in mice reveals a set of Quasi-Periodic Patterns and illustrates their relationship with the global signal. Neuroimage 180 (Pt B), 463–484.
Belloy, M.E., Shah, D., Abbas, A., Kashyap, A., Rossner, S., Van der Linden, A., Keilholz, S.D., Keliris, G.A., Verhoye, M., 2018. Quasi-periodic patterns of neural activity improve classification of alzheimer's disease in mice. Sci. Rep. 8 (1), 10024.
Bentley, W.J., Li, J.M., Snyder, A.Z., Raichle, M.E., Snyder, L.H., 2016. Oxygen level and LFP in task-positive and task-negative areas: bridging BOLD fMRI and electrophysiology. Cereb. Cortex 26 (1), 346–357.

Betzel, R.F., Avena-Koenigsberger, A., Goni, J., He, Y., de Reus, M.A., Griffa, A., Vertes, P.E., Misic, B., Thiran, J.P., Hagmann, P., van den Heuvel, M., Zuo, X.N., Bullmore, E.T., Sporns, O., 2016. Generative models of the human connectome. Neuroimage 124 (Pt A), 1054–1064.
Beul, S.F., Barbas, H., Hilgetag, C.C., 2017. A predictive structural model of the primate connectome. Sci. Rep. 7, 43176.
Birn, R.M., Cornejo, M.D., Molloy, E.K., Patriat, R., Meier, T.B., Kirk, G.R., Nair, V.A., Meyerand, M.E., Prabhakaran, V., 2014. The influence of physiological noise correction on test-retest reliability of resting-state functional connectivity. Brain Connect. 4 (7), 511–522.
Birn, R.M., Diamond, J.B., Smith, M.A., Bandettini, P.A., 2006. Separating respiratory-variation-related fluctuations from neuronal-activity-related fluctuations in fMRI. Neuroimage 31 (4), 1536–1548.
Blinder, P., Tsai, P.S., Kaufhold, J.P., Knutsen, P.M., Suhl, H., Kleinfeld, D., 2013. The cortical angiome: an interconnected vascular network with noncolumnar patterns of blood flow. Nat. Neurosci. 16 (7), 889–897.
Borowsky, I.W., Collins, R.C., 1989. Metabolic anatomy of brain: a comparison of regional capillary density, glucose metabolism, and enzyme activities. J. Comp. Neurol. 288 (3), 401–413.
Boyden, E.S., Zhang, F., Bamberg, E., Nagel, G., Deisseroth, K., 2005. Millisecond–timescale, genetically targeted optical control of neural activity. Nat. Neurosci. 8 (9), 1263–1268.
Briers, D., Duncan, D.D., Hirst, E., Kirkpatrick, S.J., Larsson, M., Steenbergen, W., Stromberg, T., Thompson, O.B., 2013. Laser speckle contrast imaging: theoretical and practical limitations. J. Biomed. Opt. 18 (6), 066018.
Bright, M.G., Whittaker, J.R., Driver, I.D., Murphy, K., 2020. Vascular physiology drives functional brain networks. Neuroimage 217, 116907.
Brinker, G., Bock, C., Busch, E., Krep, H., Hossmann, K.A., Hoehn-Berlage, M., 1999. Simultaneous recording of evoked potentials and T2*-weighted MR images during somatosensory stimulation of rat. Magn. Reson. Med. 41 (3), 469–473.
Brydges, N.M., Whalley, H.C., Jansen, M.A., Merrifield, G.D., Wood, E.R., Lawrie, S.M., Wynne, S.M., Day, M., Fleetwood-Walker, S., Steele, D., Marshall, I., Hall, J., Holmes, M.C., 2013. Imaging conditioned fear circuitry using awake rodent fMRI. PLoS One 8 (1), e54197.
Brynildsen, J.K., Hsu, L.M., Ross, T.J., Stein, E.A., Yang, Y., Lu, H., 2017. Physiological characterization of a robust survival rodent fMRI method. Magn. Reson. Imaging 35, 54–60.
Buffalo, E.A., Fries, P., Landman, R., Buschman, T.J., Desimone, R., 2011. Laminar differences in gamma and alpha coherence in the ventral stream. Proc. Natl. Acad. Sci. U. S. A. 108 (27), 11262–11267.
Bullmore, E., Sporns, O., 2012. The economy of brain network organization. Nat. Rev. Neurosci. 13 (5), 336–349.
Buxton, R.B., Wong, E.C., Frank, L.R., 1998. Dynamics of blood flow and oxygenation changes during brain activation: the balloon model. Magn. Reson. Med. 39 (6), 855–864.
Cabral, J., Hugues, E., Sporns, O., Deco, G., 2011. Role of local network oscillations in resting-state functional connectivity. Neuroimage 57 (1), 130–139.
Cabral, J., Kringelbach, M.L., Deco, G., 2017. Functional connectivity dynamically evolves on multiple time-scales over a static structural connectome: Models and mechanisms. Neuroimage 160, 84–96.
Campbell, E.J., Marchant, N.J., 2018. The use of chemogenetics in behavioural neuroscience: receptor variants, targeting approaches and caveats. Br. J. Pharmacol. 175 (7), 994–1003.
Cao, J., Lu, K.H., Oleson, S.T., Phillips, R.J., Jaffey, D., Hendren, C.L., Powley, T.L., Liu, Z., 2019. Gastric stimulation drives fast BOLD responses of neural origin. Neuroimage 197, 200–211.
Cassot, F., Lauwers, F., Fouard, C., Prohaska, S., Lauwers-Cances, V., 2006. A novel three--dimensional computer-assisted method for a quantitative study of microvascular networks of the human cerebral cortex. Microcirculation 13 (1), 1–18.
Cauli, B., Hamel, E., 2018. Brain Perfusion and Astrocytes. Trends Neurosci. 41 (7), 409–413.
Chaimow, D., Yacoub, E., Ugurbil, K., Shmuel, A., 2018. Spatial specificity of the functional MRI blood oxygenation response relative to neuronal activity. Neuroimage 164, 32–47.
Chan, A.W., Mohajerani, M.H., LeDue, J.M., Wang, Y.T., Murphy, T.H., 2015. Mesoscale infraslow spontaneous membrane potential fluctuations recapitulate high-frequency activity cortical motifs. Nat. Commun. 6, 7738.
Chan, R.W., Leong, A.T.L., Ho, L.C., Gao, P.P., Wong, E.C., Dong, C.M., Wang, X., He, J., Chan, Y.S., Lim, L.W., Wu, E.X., 2017. Low-frequency hippocampal-cortical activity drives brain-wide resting-state functional MRI connectivity. Proc. Natl. Acad. Sci. U. S. A. 114 (33), E6972–E6981.
Chang, C., Cunningham, J.P., Glover, G.H., 2009. Influence of heart rate on the BOLD signal: the cardiac response function. Neuroimage 44 (3), 857–869.
Chang, C., Leopold, D.A., Scholvinck, M.L., Mandelkow, H., Picchioni, D., Liu, X., Ye, F.Q., Turchi, J.N., Duyn, J.H., 2016. Tracking brain arousal fluctuations with fMRI. Proc. Natl. Acad. Sci. U. S. A. 113 (16), 4518–4523.
Chang, C., Liu, Z., Chen, M.C., Liu, X., Duyn, J.H., 2013a. EEG correlates of time-varying BOLD functional connectivity. Neuroimage 72, 227–236.
Chang, C., Metzger, C.D., Glover, G.H., Duyn, J.H., Heinze, H.J., Walter, M., 2013b. Association between heart rate variability and fluctuations in resting-state functional connectivity. Neuroimage 68, 93–104.
Chang, P.C., Procissi, D., Bao, Q., Centeno, M.V., Baria, A., Apkarian, A.V., 2016. Novel method for functional brain imaging in awake minimally restrained rats. J. Neurophysiol. 116 (1), 61–80.
Chen, J.E., Glover, G.H., 2015. BOLD fractional contribution to resting-state functional connectivity above 0.1 Hz. Neuroimage 107, 207–218.
Chen, J.E., Lewis, L.D., Chang, C., Tian, Q., Fultz, N.E., Ohringer, N.A., Rosen, B.R., Polimeni, J.R., 2020. Resting-state "physiological networks. Neuroimage 213, 116707.
Chen, S., Langley, J., Chen, X., Hu, X., 2016. Spatiotemporal Modeling of Brain Dynamics Using Resting-State Functional Magnetic Resonance Imaging with Gaussian Hidden Markov Model. Brain Connect. 6 (4), 326–334.
Chen, X., Sobczak, F., Chen, Y., Jiang, Y., Qian, C., Lu, Z., Ayata, C., Logothetis, N.K., Yu, X., 2019. Mapping optogenetically-driven single-vessel fMRI with concurrent neuronal calcium recordings in the rat hippocampus. Nat. Commun. 10 (1), 5239.
Chen, Y., Pais-Roldan, P., Chen, X., Frosz, M.H., Yu, X., 2019. MRI-guided robotic arm drives optogenetic fMRI with concurrent Ca(2+) recording. Nat. Commun. 10 (1), 2536.
Chernov, M., Roe, A.W., 2014. Infrared neural stimulation: a new stimulation tool for central nervous system applications. Neurophotonics 1 (1), 011011.
Chuang, K.H., Lee, H.L., Li, Z., Chang, W.T., Nasrallah, F.A., Yeow, L.Y., Singh, K., 2019. Evaluation of nuisance removal for functional MRI of rodent brain. Neuroimage 188, 694–709.
Coletta, L., Pagani, M., Whitesell, J.D., Harris, J.A., Bernhardt, B., Gozzi, A., 2020. Network structure of the mouse brain connectome with voxel resolution. Sci. Adv. 6 (51).
Cordes, D., Haughton, V.M., Arfanakis, K., Carew, J.D., Turski, P.A., Moritz, C.H., Quigley, M.A., Meyerand, M.E., 2001. Frequencies contributing to functional connectivity in the cerebral cortex in "resting-state" data. AJNR Am. J. Neuroradiol. 22 (7), 1326–1333.
Covic, E.N., Sherman, S.M., 2011. Synaptic properties of connections between the primary and secondary auditory cortices in mice. Cereb. Cortex 21 (11), 2425–2441.
Custo, A., Van De Ville, D., Wells, W.M., Tomescu, M.I., Brunet, D., Michel, C.M., 2017. Electroencephalographic Resting-State Networks: Source Localization of Microstates. Brain Connect. 7 (10), 671–682.
Daigle, T.L., Madisen, L., Hage, T.A., Valley, M.T., Knoblich, U., Larsen, R.S., Takeno, M.M., Huang, L., Gu, H., Larsen, R., Mills, M., Bosma-Moody, A., Siverts, L.A., Walker, M., Graybuck, L.T., Yao, Z., Fong, O., Nguyen, T.N., Garren, E., Lenz, G.H., Chavarha, M., Pendergraft, J., Harrington, J., Hirokawa, K.E., Harris, J.A., Nicovich, P.R., McGraw, M.J., Ollerenshaw, D.R., Smith, K.A., Baker, C.A., Ting, J.T., Sunkin, S.M., Lecoq, J., Lin, M.Z., Boyden, E.S., Murphy, G.J., da Costa, N.M., Waters, J., Li, L., Tasic, B., Zeng, H., 2018. A suite of transgenic driver and reporter mouse lines with enhanced brain-Cell-type targeting and functionality. Cell 174 (2), 465–480 e422.
Dana, H., Sun, Y., Mohar, B., Hulse, B.K., Kerlin, A.M., Hasseman, J.P., Tsegaye, G., Tsang, A., Wong, A., Patel, R., Macklin, J.J., Chen, Y., Konnerth, A., Jayaraman, V., Looger, L.L., Schreiter, E.R., Svoboda, K., Kim, D.S., 2019. High-performance calcium sensors for imaging activity in neuronal populations and microcompartments. Nat. Methods 16 (7), 649–657.
David, O., Guillemain, I., Saillet, S., Reyt, S., Deransart, C., Segebarth, C., Depaulis, A., 2008. Identifying neural drivers with functional MRI: an electrophysiological validation. PLoS Biol. 6 (12), 2683–2697.
de la Cruz, F., Schumann, A., Kohler, S., Bar, K.J., Wagner, G., 2017. Impact of the heart rate on the shape of the cardiac response function. Neuroimage 162, 214–225.
Decot, H.K., Namboodiri, V.M., Gao, W., McHenry, J.A., Jennings, J.H., Lee, S.H., Kantak, P.A., Jill Kao, Y.C., Das, M., Witten, I.B., Deisseroth, K., Shih, Y.I., Stuber, G.D., 2017. Coordination of brain-wide activity dynamics by dopaminergic neurons. Neuropsychopharmacology 42 (3), 615–627.
Desai, M., Kahn, I., Knoblich, U., Bernstein, J., Atallah, H., Yang, A., Kopell, N., Buckner, R.L., Graybiel, A.M., Moore, C.I., Boyden, E.S., 2011. Mapping brain networks in awake mice using combined optical neural control and fMRI. J. Neurophysiol. 105 (3), 1393–1405.
Devonshire, I.M., Papadakis, N.G., Port, M., Berwick, J., Kennerley, A.J., Mayhew, J.E., Overton, P.G., 2012. Neurovascular coupling is brain region-dependent. Neuroimage 59 (3), 1997–2006.
Diaz-Parra, A., Osborn, Z., Canals, S., Moratal, D., Sporns, O., 2017. Structural and functional, empirical and modeled connectivity in the cerebral cortex of the rat. Neuroimage 159, 170–184.
Disney, A.A., Higley, M.J., 2020. Diverse Spatiotemporal Scales of Cholinergic Signaling in the Neocortex. J. Neurosci. 40 (4), 720–725.
Dizeux, A., Gesnik, M., Ahnine, H., Blaize, K., Arcizet, F., Picaud, S., Sahel, J.A., Deffieux, T., Pouget, P., Tanter, M., 2019. Functional ultrasound imaging of the brain reveals propagation of task-related brain activity in behaving primates. Nat. Commun. 10 (1), 1400.
Douglas, R.J., Martin, K.A., 1991. A functional microcircuit for cat visual cortex. J. Physiol. 440, 735–769.
Drew, P.J., Duyn, J.H., Golanov, E., Kleinfeld, D., 2008. Finding coherence in spontaneous oscillations. Nat. Neurosci. 11 (9), 991–993.
Drew, P.J., Mateo, C., Turner, K.L., Yu, X., Kleinfeld, D., 2020. Ultra-slow oscillations in fMRI and resting-state connectivity: neuronal and vascular contributions and technical confounds. Neuron 107 (5), 782–804.
Duvernoy, H.M., Delon, S., Vannson, J.L., 1981. Cortical blood vessels of the human brain. Brain Res. Bull. 7 (5), 519–579.
Dzirasa, K., Phillips, H.W., Sotnikova, T.D., Salahpour, A., Kumar, S., Gainetdinov, R.R., Caron, M.G., Nicolelis, M.A., 2010. Noradrenergic control of cortico-striato-thalamic and mesolimbic cross-structural synchrony. J. Neurosci. 30 (18), 6387–6397.
Echagarruga, C.T., Gheres, K.W., Norwood, J.N., Drew, P.J., 2020. nNOS-expressing interneurons control basal and behaviorally evoked arterial dilation in somatosensory cortex of mice. Elife 9, e60533. doi:10.7554/eLife.60533, PMID: 33016877.
Ercsey-Ravasz, M., Markov, N.T., Lamy, C., Van Essen, D.C., Knoblauch, K., Toroczkai, Z., Kennedy, H., 2013. A predictive network model of cerebral cortical connectivity based on a distance rule. Neuron 80 (1), 184–197.
Falahpour, M., Chang, C., Wong, C.W., Liu, T.T., 2018. Template-based prediction of vigilance fluctuations in resting-state fMRI. Neuroimage 174, 317–327.

Fernandez-Klett, F., Offenhauser, N., Dirnagl, U., Priller, J., Lindauer, U., 2010. Pericytes in capillaries are contractile in vivo, but arterioles mediate functional hyperemia in the mouse brain. Proc. Natl. Acad. Sci. U. S. A. 107 (51), 22290–22295.
Ferrier, J., Tiran, E., Deffieux, T., Tanter, M., Lenkei, Z., 2020. Functional imaging evidence for task-induced deactivation and disconnection of a major default mode network hub in the mouse brain. Proc. Natl. Acad. Sci. U. S. A. 117 (26), 15270–15280.
Finn, E.S., Huber, L., Jangraw, D.C., Molfese, P.J., Bandettini, P.A., 2019. Layer-dependent activity in human prefrontal cortex during working memory. Nat. Neurosci. 22 (10), 1687–1695.
Fleming, S., Thompson, M., Stevens, R., Heneghan, C., Pluddemann, A., Maconochie, I., Tarassenko, L., Mant, D., 2011. Normal ranges of heart rate and respiratory rate in children from birth to 18 years of age: a systematic review of observational studies. Lancet 377 (9770), 1011–1018.
Fox, M.D., Snyder, A.Z., Vincent, J.L., Corbetta, M., Van Essen, D.C., Raichle, M.E., 2005. The human brain is intrinsically organized into dynamic, anticorrelated functional networks. Proc. Natl. Acad. Sci. U. S. A. 102 (27), 9673–9678.
Fox, M.D., Zhang, D., Snyder, A.Z., Raichle, M.E., 2009. The global signal and observed anticorrelated resting state brain networks. J. Neurophysiol. 101 (6), 3270–3283.
Friston, K.J., Mechelli, A., Turner, R., Price, C.J., 2000. Nonlinear responses in fMRI: the Balloon model, Volterra kernels, and other hemodynamics. Neuroimage 12 (4), 466–477.
Fukuda, M., Moon, C.H., Wang, P., Kim, S.G., 2006. Mapping iso-orientation columns by contrast agent-enhanced functional magnetic resonance imaging: reproducibility, specificity, and evaluation by optical imaging of intrinsic signal. J. Neurosci. 26 (46), 11821–11832.
Fukunaga, M., Horovitz, S.G., van Gelderen, P., de Zwart, J.A., Jansma, J.M., Ikonomidou, V.N., Chu, R., Deckers, R.H., Leopold, D.A., Duyn, J.H., 2006. Large-amplitude, spatially correlated fluctuations in BOLD fMRI signals during extended rest and early sleep stages. Magn. Reson. Imaging 24 (8), 979–992.
Fultz, N.E., Bonmassar, G., Setsompop, K., Stickgold, R.A., Rosen, B.R., Polimeni, J.R., Lewis, L.D., 2019. Coupled electrophysiological, hemodynamic, and cerebrospinal fluid oscillations in human sleep. Science 366 (6465), 628–631.
Gentet, L.J., Avermann, M., Matyas, F., Staiger, J.F., Petersen, C.C., 2010. Membrane potential dynamics of GABAergic neurons in the barrel cortex of behaving mice. Neuron 65 (3), 422–435.
Gentet, L.J., Kremer, Y., Taniguchi, H., Huang, Z.J., Staiger, J.F., Petersen, C.C., 2012. Unique functional properties of somatostatin-expressing GABAergic neurons in mouse barrel cortex. Nat. Neurosci. 15 (4), 607–612.
Goense, J.B., Logothetis, N.K., 2006. Laminar specificity in monkey V1 using high-resolution SE-fMRI. Magn. Reson. Imaging 24 (4), 381–392.
Golanov, E.V., Reis, D.J., 1996. Contribution of oxygen-sensitive neurons of the rostral ventrolateral medulla to hypoxic cerebral vasodilatation in the rat. J. Physiol. 495 (Pt 1), 201–216.
Gonchar, Y., Wang, Q., Burkhalter, A., 2007. Multiple distinct subtypes of GABAergic neurons in mouse visual cortex identified by triple immunostaining. Front. Neuroanat 1, 3.
Goulas, A., Uylings, H.B., Hilgetag, C.C., 2017. Principles of ipsilateral and contralateral cortico-cortical connectivity in the mouse. Brain Struct. Funct. 222 (3), 1281–1295.
Grandjean, J., Corcoba, A., Kahn, M.C., Upton, A.L., Deneris, E.S., Seifritz, E., Helmchen, F., Mann, E.O., Rudin, M., Saab, B.J., 2019. A brain-wide functional map of the serotonergic responses to acute stress and fluoxetine. Nat. Commun. 10 (1), 350.
Griffanti, L., Douaud, G., Bijsterbosch, J., Evangelisti, S., Alfaro-Almagro, F., Glasser, M.F., Duff, E.P., Fitzgibbon, S., Westphal, R., Carone, D., Beckmann, C.F., Smith, S.M., 2017. Hand classification of fMRI ICA noise components. Neuroimage 154, 188–205.
Grinvald, A., Lieke, E., Frostig, R.D., Gilbert, C.D., Wiesel, T.N., 1986. Functional architecture of cortex revealed by optical imaging of intrinsic signals. Nature 324 (6095), 361–364.
Grooms, J.K., Thompson, G.J., Pan, W.J., Billings, J., Schumacher, E.H., Epstein, C.M., Keilholz, S.D., 2017. Infraslow electroencephalographic and dynamic resting state network activity. Brain Connect. 7 (5), 265–280.
Grubb, S., Lauritzen, M., Aalkjaer, C., 2021. Brain capillary pericytes and neurovascular coupling. Comp. Biochem. Physiol. A Mol. Integr. Physiol. 254, 110893.
Gu, X., Chen, W., Volkow, N.D., Koretsky, A.P., Du, C., Pan, Y., 2018. Synchronized Astrocytic Ca(2+) responses in neurovascular coupling during somatosensory stimulation and for the resting state. Cell Rep. 23 (13), 3878–3890.
Haimovici, A., Tagliazucchi, E., Balenzuela, P., Chialvo, D.R., 2013. Brain organization into resting state networks emerges at criticality on a model of the human connectome. Phys. Rev. Lett. 110 (17), 178101.
Han, Z., Chen, W., Chen, X., Zhang, K., Tong, C., Zhang, X., Li, C.T., Liang, Z., 2019. Awake and behaving mouse fMRI during Go/No-Go task. Neuroimage 188, 733–742.
Harris, J.A., Mihalas, S., Hirokawa, K.E., Whitesell, J.D., Choi, H., Bernard, A., Bohn, P., Caldejon, S., Casal, L., Cho, A., Feiner, A., Feng, D., Gaudreault, N., Gerfen, C.R., Graddis, N., Groblewski, P.A., Henry, A.M., Ho, A., Howard, R., Knox, J.E., Kuan, L., Kuang, X., Lecoq, J., Lesnar, P., Li, Y., Luviano, J., McConoughey, S., Mortrud, M.T., Naeemi, M., Ng, L., Oh, S.W., Ouellette, B., Shen, E., Sorensen, S.A., Wakeman, W., Wang, Q., Wang, Y., Williford, A., Phillips, J.W., Jones, A.R., Koch, C., Zeng, H., 2019. Hierarchical organization of cortical and thalamic connectivity. Nature 575 (7781), 195–202.
Hartmann, D.A., Berthiaume, A.A., Grant, R.I., Harrill, S.A., Koski, T., Tieu, T., McDowell, K.P., Faino, A.V., Kelly, A.L., Shih, A.Y., 2021. Brain capillary pericytes exert a substantial but slow influence on blood flow. Nat. Neurosci. 24 (5), 633–645. doi:10.1038/s41593-020-00793-2, Epub 2021 Feb 18. PMID: 33603231.
Hartmann, D.A., Underly, R.G., Grant, R.I., Watson, A.N., Lindner, V., Shih, A.Y., 2015. Pericyte structure and distribution in the cerebral cortex revealed by high-resolution imaging of transgenic mice. Neurophotonics 2 (4), 041402.
Haufler, D., Pare, D., 2019. Detection of multiway gamma coordination reveals how frequency mixing shapes neural dynamics. Neuron 101 (4), 603–614 e606.
He, B.J., Snyder, A.Z., Zempel, J.M., Smyth, M.D., Raichle, M.E., 2008. Electrophysiological correlates of the brain's intrinsic large-scale functional architecture. Proc. Natl. Acad. Sci. U. S. A. 105 (41), 16039–16044.
He, Y., Wang, M., Chen, X., Pohmann, R., Polimeni, J.R., Scheffler, K., Rosen, B.R., Kleinfeld, D., Yu, X., 2018. Ultra-slow single-vessel BOLD and CBV-Based fMRI spatiotemporal dynamics and their correlation with neuronal intracellular calcium signals. Neuron 97 (4), 925–939 e925.
He, Y., Wang, M.S., Chen, X.M., Pohmann, R., Polimeni, J.R., Scheffler, K., Rosen, B.R., Kleinfeld, D., Yu, X., 2018. Ultra-slow single-vessel BOLD and CBV-based fMRI spatiotemporal dynamics and their correlation with neuronal intracellular calcium signals. Neuron 97 (4), 925 -+.
Helmchen, F., Denk, W., 2005. Deep tissue two-photon microscopy. Nat. Methods 2 (12), 932–940.
Hill, R.A., Tong, L., Yuan, P., Murikinati, S., Gupta, S., Grutzendler, J., 2015. Regional blood flow in the normal and ischemic brain is controlled by arteriolar smooth muscle cell contractility and not by capillary pericytes. Neuron 87 (1), 95–110.
Hillman, E.M., 2007. Optical brain imaging in vivo: techniques and applications from animal to man. J. Biomed. Opt. 12 (5), 051402.
Hiltunen, T., Kantola, J., Abou Elseoud, A., Lepola, P., Suominen, K., Starck, T., Nikkinen, J., Remes, J., Tervonen, O., Palva, S., Kiviniemi, V., Palva, J.M., 2014. Infra-slow EEG fluctuations are correlated with resting-state network dynamics in fMRI. J. Neurosci. 34 (2), 356–362.
Hooks, B.M., Mao, T., Gutnisky, D.A., Yamawaki, N., Svoboda, K., Shepherd, G.M., 2013. Organization of cortical and thalamic input to pyramidal neurons in mouse motor cortex. J. Neurosci. 33 (2), 748–760.
Hori, Y., Schaeffer, D.J., Gilbert, K.M., Hayrynen, L.K., Clery, J.C., Gati, J.S., Menon, R.S., Everling, S., 2020. Comparison of resting-state functional connectivity in marmosets with tracer-based cellular connectivity. Neuroimage 204, 116241.
Horton, J.C., Adams, D.L., 2005. The cortical column: a structure without a function. Philos. Trans. R. Soc. Lond. B Biol. Sci. 360 (1456), 837–862.
Horton, N.G., Wang, K., Kobat, D., Clark, C.G., Wise, F.W., Schaffer, C.B., Xu, C., 2013. In vivo three-photon microscopy of subcortical structures within an intact mouse brain. Nat Photonics 7 (3).
Hsu, L.M., Liang, X., Gu, H., Brynildsen, J.K., Stark, J.A., Ash, J.A., Lin, C.P., Lu, H., Rapp, P.R., Stein, E.A., Yang, Y., 2016. Constituents and functional implications of the rat default mode network. Proc. Natl. Acad. Sci. U. S. A. 113 (31), E4541–E4547.
Huber, L., Handwerker, D.A., Jangraw, D.C., Chen, G., Hall, A., Stuber, C., Gonzalez–Castillo, J., Ivanov, D., Marrett, S., Guidi, M., Goense, J., Poser, B.A., Bandettini, P.A., 2017. High-Resolution CBV-fMRI Allows Mapping of Laminar Activity and Connectivity of Cortical Input and Output in Human M1. Neuron 96 (6), 1253–1263 e1257.
Hudetz, A.G., Liu, X., Pillay, S., 2015. Dynamic repertoire of intrinsic brain states is reduced in propofol-induced unconsciousness. Brain Connect. 5 (1), 10–22.
Huo, B.X., Smith, J.B., Drew, P.J., 2014. Neurovascular coupling and decoupling in the cortex during voluntary locomotion. J. Neurosci. 34 (33), 10975–10981.
Iordanova, B., Vazquez, A.L., Poplawsky, A.J., Fukuda, M., Kim, S.G., 2015. Neural and hemodynamic responses to optogenetic and sensory stimulation in the rat somatosensory cortex. J. Cereb. Blood Flow Metab. 35 (6), 922–932.
Ji, X., Ferreira, T., Friedman, B., Liu, R., Liechty, H., Bas, E., Chandrashekar, J., Kleinfeld, D., 2021. Brain microvasculature has a common topology with local differences in geometry that match metabolic load. Neuron 109 (7), 1168–1187 e13. doi:10.1016/j.neuron.2021.02.006. Epub 2021 Mar 2..
Kahn, I., Knoblich, U., Desai, M., Bernstein, J., Graybiel, A.M., Boyden, E.S., Buckner, R.L., Moore, C.I., 2013. Optogenetic drive of neocortical pyramidal neurons generates fMRI signals that are correlated with spiking activity. Brain Res. 1511, 33–45.
Kalthoff, D., Seehafer, J.U., Po, C., Wiedermann, D., Hoehn, M., 2011. Functional connectivity in the rat at 11.7T: impact of physiological noise in resting state fMRI. Neuroimage 54 (4), 2828–2839.
Kannurpatti, S.S., Biswal, B.B., Kim, Y.R., Rosen, B.R., 2008. Spatio-temporal characteristics of low-frequency BOLD signal fluctuations in isoflurane-anesthetized rat brain. Neuroimage 40 (4), 1738–1747.
Kashyap, A., Keilholz, S., 2019. Dynamic properties of simulated brain network models and empirical resting-state data. Netw. Neurosci. 3 (2), 405–426.
Kashyap, A., Keilholz, S., 2020. Brain network constraints and recurrent neural networks reproduce unique trajectories and state transitions seen over the span of minutes in resting-state fMRI. Netw. Neurosci. 4 (2), 448–466.
Kashyap, S., Ivanov, D., Havlicek, M., Sengupta, S., Poser, B.A., Uludag, K., 2018. Resolving laminar activation in human V1 using ultra-high spatial resolution fMRI at 7T. Sci Rep 8 (1), 17063.
Katzel, D., Zemelman, B.V., Buetfering, C., Wolfel, M., Miesenbock, G., 2011. The columnar and laminar organization of inhibitory connections to neocortical excitatory cells. Nat. Neurosci. 14 (1), 100–107.
Kay, K., Jamison, K.W., Vizioli, L., Zhang, R., Margalit, E., Ugurbil, K., 2019. A critical assessment of data quality and venous effects in sub-millimeter fMRI. Neuroimage 189, 847–869.
Kay, K., Jamison, K.W., Zhang, R.Y., Ugurbil, K., 2020. A temporal decomposition method for identifying venous effects in task-based fMRI. Nat. Methods 17 (10), 1033–1039.
Keilholz, S.D., Magnuson, M.E., Pan, W.J., Willis, M., Thompson, G.J., 2013. Dynamic properties of functional connectivity in the rodent. Brain Connect. 3 (1), 31–40.
Keilholz, S.D., Pan, W.J., Billings, J., Nezafati, M., Shakil, S., 2017. Noise and non-neuronal contributions to the BOLD signal: applications to and insights from animal studies. Neuroimage 154, 267–281.
Keilholz, S.D., Silva, A.C., Raman, M., Merkle, H., Koretsky, A.P., 2004. Functional MRI of the rodent somatosensory pathway using multislice echo planar imaging. Magn. Reson. Med. 52 (1), 89–99.

Keilholz, S.D., Silva, A.C., Raman, M., Merkle, H., Koretsky, A.P., 2006. BOLD and CBV-weighted functional magnetic resonance imaging of the rat somatosensory system. Magn. Reson. Med. 55 (2), 316–324.
Kida, I., Kennan, R.P., Rothman, D.L., Behar, K.L., Hyder, F., 2000. High-resolution CMR(O_2) mapping in rat cortex: a multiparametric approach to calibration of BOLD image contrast at 7 Tesla. J. Cereb. Blood Flow Metab. 20 (5), 847–860.
Kim, D.S., Duong, T.Q., Kim, S.G., 2000. High-resolution mapping of iso-orientation columns by fMRI. Nat. Neurosci. 3 (2), 164–169.
Kim, J.H., Jung, A.H., Jeong, D., Choi, I., Kim, K., Shin, S., Kim, S.J., Lee, S.H., 2016. Selectivity of neuromodulatory projections from the basal forebrain and locus ceruleus to primary sensory cortices. J. Neurosci. 36 (19), 5314–5327.
Kim, Y., Yang, G.R., Pradhan, K., Venkataraju, K.U., Bota, M., Garcia Del Molino, L.C., Fitzgerald, G., Ram, K., He, M., Levine, J.M., Mitra, P., Huang, Z.J., Wang, X.J., Osten, P., 2017. Brain-wide maps reveal stereotyped Cell-type-based cortical architecture and subcortical sexual dimorphism. Cell 171 (2), 456–469 e422.
King, J.A., Garelick, T.S., Brevard, M.E., Chen, W., Messenger, T.L., Duong, T.Q., Ferris, C.F., 2005. Procedure for minimizing stress for fMRI studies in conscious rats. J Neurosci Methods 148 (2), 154–160.
Kleinfeld, D., Luan, L., Mitra, P.P., Robinson, J.T., Sarpeshkar, R., Shepard, K., Xie, C., Harris, T.D., 2019. Can one concurrently record electrical spikes from every neuron in a mammalian brain? Neuron 103 (6), 1005–1015.
Kocharyan, A., Fernandes, P., Tong, X.K., Vaucher, E., Hamel, E., 2008. Specific subtypes of cortical GABA interneurons contribute to the neurovascular coupling response to basal forebrain stimulation. J. Cereb. Blood Flow Metab. 28 (2), 221–231.
Koenigsberger, M., Sauser, R., Beny, J.L., Meister, J.J., 2006. Effects of arterial wall stress on vasomotion. Biophys. J. 91 (5), 1663–1674.
Kozberg, M.G., Hillman, E.M., 2016. Neurovascular coupling develops alongside neural circuits in the postnatal brain. Neurogenesis 3 (1), e1244439 Austin.
Krawchuk, M.B., Ruff, C.F., Yang, X., Ross, S.E., Vazquez, A.L., 2020. Optogenetic assessment of VIP, PV, SOM and NOS inhibitory neuron activity and cerebral blood flow regulation in mouse somato-sensory cortex. J. Cereb. Blood Flow Metab. 40 (7), 1427–1440.
Kubota, Y., Karube, F., Nomura, M., Kawaguchi, Y., 2016. The Diversity of Cortical Inhibitory Synapses. Front. Neural Circuits 10, 27.
Kucyi, A., Daitch, A., Raccah, O., Zhao, B., Zhang, C., Esterman, M., Zeineh, M., Halpern, C.H., Zhang, K., Zhang, J., Parvizi, J., 2020. Electrophysiological dynamics of antagonistic brain networks reflect attentional fluctuations. Nat. Commun. 11 (1), 325.
Kuga, N., Sasaki, T., Takahara, Y., Matsuki, N., Ikegaya, Y., 2011. Large-scale calcium waves traveling through astrocytic networks in vivo. J. Neurosci. 31 (7), 2607–2614.
Kundu, P., Santin, M.D., Bandettini, P.A., Bullmore, E.T., Petiet, A., 2014. Differentiating BOLD and non-BOLD signals in fMRI time series from anesthetized rats using multi-echo EPI at 11.7 T. Neuroimage 102 (Pt 2), 861–874.
Kura, S., Xie, H., Fu, B., Ayata, C., Boas, D.A., Sakadzic, S., 2018. Intrinsic optical signal imaging of the blood volume changes is sufficient for mapping the resting state functional connectivity in the rodent cortex. J. Neural Eng. 15 (3), 035003.
Lacroix, A., Toussay X., Anenberg E., Lecrux C., Ferreiros N., Karagiannis A., Plaisier F., Chausson P., Jarlier F., Burgess S.A., Hillman E.M., Tegeder I., Murphy T.H., Hamel E. and Cauli B. (2015). "COX-2-derived prostaglandin E2 produced by pyramidal neurons contributes to neurovascular coupling in the rodent cerebral cortex." J. Neurosci. 35(34): 11791–11810.
Lake, E.M.R., Ge, X., Shen, X., Herman, P., Hyder, F., Cardin, J.A., Higley, M.J., Scheinost, D., Papademetris, X., Crair, M.C., Constable, R.T., 2020. Simultaneous cortex-wide fluorescence Ca(2+) imaging and whole-brain fMRI. Nat. Methods 17 (12), 1262–1271.
Lecrux, C., Hamel, E., 2016. Neuronal networks and mediators of cortical neurovascular coupling responses in normal and altered brain states. Philos. Trans. R. Soc. Lond. B Biol. Sci. 371 (1705), 20150350. doi:10.1098/rstb.2015.0350.
Lecrux, C., Sandoe, C.H., Neupane, S., Kropf, P., Toussay, X., Tong, X.K., Lacalle-Aurioles, M., Shmuel, A., Hamel, E., 2017. Impact of altered cholinergic tones on the neurovascular coupling response to whisker stimulation. J. Neurosci. 37 (6), 1518–1531.
Lecrux, C., Toussay, X., Kocharyan, A., Fernandes, P., Neupane, S., Levesque, M., Plaisier, F., Shmuel, A., Cauli, B., Hamel, E., 2011. Pyramidal neurons are "neurogenic hubs" in the neurovascular coupling response to whisker stimulation. J. Neurosci. 31 (27), 9836–9847.
Ledo, A., Lourenco, C.F., Laranjinha, J., Gerhardt, G.A., Barbosa, R.M., 2017. Combined *in vivo* amperometric oximetry and electrophysiology in a single sensor: a tool for epilepsy research. Anal. Chem. 89 (22), 12383–12390.
Lee, J.H., Durand, R., Gradinaru, V., Zhang, F., Goshen, I., Kim, D.S., Fenno, L.E., Ramakrishnan, C., Deisseroth, K., 2010. Global and local fMRI signals driven by neurons defined optogenetically by type and wiring. Nature 465 (7299), 788–792.
Lee, J., Stile, C.L., Bice, A.R., Rosenthal, Z.P., Yan, P., Snyder, A.Z., Lee, J.M., Bauer, A.Q., 2021. Opposed hemodynamic responses following increased excitation and parvalbumin-based inhibition. J. Cereb. Blood Flow Metab. 41 (4), 841–856. doi:10.1177/0271678X20930831, Epub 2020 Jun 17. PMID: 33736512.
Lee, L., Boorman, L., Glendenning, E., Christmas, C., Sharp, P., Redgrave, P., Shabir, O., Bracci, E., Berwick, J., Howarth, C., 2020. Key Aspects of Neurovascular Control Mediated by Specific Populations of Inhibitory Cortical Interneurons. Cereb. Cortex 30 (4), 2452–2464.
Lehto, L.J., Idiyatullin, D., Zhang, J., Utecht, L., Adriany, G., Garwood, M., Grohn, O., Michaeli, S., Mangia, S., 2017. MB-SWIFT functional MRI during deep brain stimulation in rats. Neuroimage 159, 443–448.
Leong, A.T., Chan, R.W., Gao, P.P., Chan, Y.S., Tsia, K.K., Yung, W.H., Wu, E.X., 2016. Long-range projections coordinate distributed brain-wide neural activity with a specific spatiotemporal profile. Proc. Natl. Acad. Sci. U. S. A. 113 (51), E8306–E8315.
Li, J.M., Bentley, W.J., Snyder, L.H., 2015. Functional connectivity arises from a slow rhythmic mechanism. Proc. Natl. Acad. Sci. U. S. A. 112 (19), E2527–E2535.
Li, S., Hu, N., Zhang, W., Tao, B., Dai, J., Gong, Y., Tan, Y., Cai, D., Lui, S., 2019. Dysconnectivity of multiple brain networks in schizophrenia: a meta-analysis of resting-state functional connectivity. Front. Psychiatry 10, 482.
Li, X., Yu, B., Sun, Q., Zhang, Y., Ren, M., Zhang, X., Li, A., Yuan, J., Madisen, L., Luo, Q., Zeng, H., Gong, H., Qiu, Z., 2018. Generation of a whole-brain atlas for the cholinergic system and mesoscopic projectome analysis of basal forebrain cholinergic neurons. Proc. Natl. Acad. Sci. U. S. A. 115 (2), 415–420.
Liang, X., Hsu, L.M., Lu, H., Sumiyoshi, A., He, Y., Yang, Y., 2018. The rich-club organization in rat functional brain network to balance between communication cost and efficiency. Cereb. Cortex 28 (3), 924–935.
Liegeois, R., Ziegler, E., Phillips, C., Geurts, P., Gomez, F., Bahri, M.A., Yeo, B.T., Soddu, A., Vanhaudenhuyse, A., Laureys, S., Sepulchre, R., 2016. Cerebral functional connectivity periodically (de)synchronizes with anatomical constraints. Brain Struct. Funct. 221 (6), 2985–2997.
Liguz-Lecznar, M., Urban-Ciecko, J., Kossut, M., 2016. Somatostatin and somatostatin–containing neurons in shaping neuronal activity and plasticity. Front. Neural Circuits 10, 48.
Lindvall, O., Bjorklund, A., Divac, I., 1978. Organization of catecholamine neurons projecting to the frontal cortex in the rat. Brain Res. 142 (1), 1–24.
Liu, R., Li, Z., Marvin, J.S., Kleinfeld, D., 2019. Direct wavefront sensing enables functional imaging of infragranular axons and spines. Nat. Methods 16 (7), 615–618.
Liu, X., Duyn, J.H., 2013. Time-varying functional network information extracted from brief instances of spontaneous brain activity. Proc. Natl. Acad. Sci. U. S. A. 110 (11), 4392–4397.
Liu, X., Yanagawa, T., Leopold, D.A., Chang, C., Ishida, H., Fujii, N., Duyn, J.H., 2015. Arousal transitions in sleep, wakefulness, and anesthesia are characterized by an orderly sequence of cortical events. Neuroimage 116, 222–231.
Logothetis, N.K., Pauls, J., Augath, M., Trinath, T., Oeltermann, A., 2001. Neurophysiological investigation of the basis of the fMRI signal. Nature 412 (6843), 150–157.
Longden, T.A., Dabertrand, F., Koide, M., Gonzales, A.L., Tykocki, N.R., Brayden, J.E., Hill-Eubanks, D., Nelson, M.T., 2017. Capillary K(+)-sensing initiates retrograde hyperpolarization to increase local cerebral blood flow. Nat. Neurosci. 20 (5), 717–726.
Lottem, E., Lorincz, M.L., Mainen, Z.F., 2016. Optogenetic activation of dorsal raphe serotonin neurons rapidly inhibits spontaneous but not odor-evoked activity in olfactory cortex. J. Neurosci. 36 (1), 7–18.
Lu, H., Zou, Q., Gu, H., Raichle, M.E., Stein, E.A., Yang, Y., 2012. Rat brains also have a default mode network. Proc. Natl. Acad. Sci. U. S. A. 109 (10), 3979–3984.
Lu, H., Zuo, Y., Gu, H., Waltz, J.A., Zhan, W., Scholl, C.A., Rea, W., Yang, Y., Stein, E.A., 2007. Synchronized delta oscillations correlate with the resting-state functional MRI signal. Proc. Natl. Acad. Sci. U. S. A. 104 (46), 18265–18269.
Lu, R., Liang, Y., Meng, G., Zhou, P., Svoboda, K., Paninski, L., Ji, N., 2020. Rapid mesoscale volumetric imaging of neural activity with synaptic resolution. Nat. Methods 17 (3), 291–294.
Lund, J.S., Angelucci, A., Bressloff, P.C., 2003. Anatomical substrates for functional columns in macaque monkey primary visual cortex. Cereb. Cortex 13 (1), 15–24.
Carandini, M, A Cagatay, N.S., Lebedeva, A, Okun, M, Pachitariu, M, Dudman, J, Dutta, B, Hantman, A, Harris, KD, Lee, A, Moser, E, O'Keefe, J, Renart, A, Svoboda, K, Hausser, M, Haesler, S, Harris, TD, 2021. Neuropixels 2.0: a miniaturized high-density probe for stable, long-term brain recordings. Science.
Ma, Y., Shaik, M.A., Kozberg, M.G., Kim, S.H., Portes, J.P., Timerman, D., Hillman, E.M., 2016. Resting-state hemodynamics are spatiotemporally coupled to synchronized and symmetric neural activity in excitatory neurons. Proc. Natl. Acad. Sci. U. S. A. 113 (52), E8463–E8471.
Mace, E., Montaldo, G., Cohen, I., Baulac, M., Fink, M., Tanter, M., 2011. Functional ultrasound imaging of the brain. Nat. Methods 8 (8), 662–664.
Magnuson, M.E., Thompson, G.J., Pan, W.J., Keilholz, S.D., 2014. Effects of severing the corpus callosum on electrical and BOLD functional connectivity and spontaneous dynamic activity in the rat brain. Brain Connect. 4 (1), 15–29.
Magri, C., Schridde, U., Murayama, Y., Panzeri, S., Logothetis, N.K., 2012. The amplitude and timing of the BOLD signal reflects the relationship between local field potential power at different frequencies. J. Neurosci. 32 (4), 1395–1407.
Majeed, W., Magnuson, M., Hasenkamp, W., Schwarb, H., Schumacher, E.H., Barsalou, L., Keilholz, S.D., 2011. Spatiotemporal dynamics of low frequency BOLD fluctuations in rats and humans. Neuroimage 54 (2), 1140–1150.
Majeed, W., Magnuson, M., Keilholz, S.D., 2009. Spatiotemporal dynamics of low frequency fluctuations in BOLD fMRI of the rat. J. Magn. Reson. Imaging 30 (2), 384–393.
Malonek, D., Grinvald, A., 1996. Interactions between electrical activity and cortical microcirculation revealed by imaging spectroscopy: implications for functional brain mapping. Science 272 (5261), 551–554.
Mandino, F., Cerri, D.H., Garin, C.M., Straathof, M., van Tilborg, G.A.F., Chakravarty, M.M., Dhenain, M., Dijkhuizen, R.M., Gozzi, A., Hess, A., Keilholz, S.D., Lerch, J.P., Shih, Y.I., Grandjean, J., 2019. Animal Functional Magnetic Resonance Imaging: Trends and Path Toward Standardization. Front. Neuroinform. 13, 78.
Mantini, D., Gerits, A., Nelissen, K., Durand, J.B., Joly, O., Simone, L., Sawamura, H., Wardak, C., Orban, G.A., Buckner, R.L., Vanduffel, W., 2011. Default mode of brain function in monkeys. J. Neurosci. 31 (36), 12954–12962.
Manwar, R., Kratkiewicz, K., Avanaki, K., 2020. Investigation of the effect of the skull in transcranial photoacoustic imaging: a preliminary *ex vivo* study. Sens. (Basel) 20 (15).
Margulies, D.S., Ghosh, S.S., Goulas, A., Falkiewicz, M., Huntenburg, J.M., Langs, G., Bezgin, G., Eickhoff, S.B., Castellanos, F.X., Petrides, M., Jefferies, E., Smallwood, J., 2016. Situating the default-mode network along a principal gradient of macroscale cortical organization. Proc. Natl. Acad. Sci. U. S. A. 113 (44), 12574–12579.

Masamoto, K., Unekawa, M., Watanabe, T., Toriumi, H., Takuwa, H., Kawaguchi, H., Kanno, I., Matsui, K., Tanaka, K.F., Tomita, Y., Suzuki, N., 2015. Unveiling astrocytic control of cerebral blood flow with optogenetics. Sci. Rep. 5, 11455.
Massimini, M., Huber, R., Ferrarelli, F., Hill, S., Tononi, G., 2004. The sleep slow oscillation as a traveling wave. J. Neurosci. 24 (31), 6862–6870.
Mateo, C., Avermann, M., Gentet, L.J., Zhang, F., Deisseroth, K., Petersen, C.C., 2011. In vivo optogenetic stimulation of neocortical excitatory neurons drives brain-state-dependent inhibition. Curr. Biol. 21 (19), 1593–1602.
Mateo, C., Knutsen, P.M., Tsai, P.S., Shih, A.Y., Kleinfeld, D., 2017. Entrainment of arteriole vasomotor fluctuations by neural activity is a basis of blood-oxygenation-level-dependent "Resting-State" connectivity. Neuron 96 (4), 936–948 e933.
Matsui, T., Murakami, T., Ohki, K., 2016. Transient neuronal coactivations embedded in globally propagating waves underlie resting-state functional connectivity. Proc. Natl. Acad. Sci. U. S. A. 113 (23), 6556–6561.
McAvoy, M.P., Tagliazucchi, E., Laufs, H., Raichle, M.E., 2019. Human non-REM sleep and the mean global BOLD signal. J. Cereb. Blood Flow Metab. 39 (11), 2210–2222.
Meir, I., Katz, Y., Lampl, I., 2018. Membrane potential correlates of network decorrelation and improved SNR by cholinergic activation in the somatosensory cortex. J. Neurosci. 38 (50), 10692–10708.
Menon, R.S., Ogawa, S., Kim, S.G., Ellermann, J.M., Merkle, H., Tank, D.W., Ugurbil, K., 1992. Functional brain mapping using magnetic resonance imaging. Signal changes accompanying visual stimulation. Invest. Radiol. 27 (Suppl 2), S47–S53.
Messe, A., 2020. Parcellation influence on the connectivity-based structure-function relationship in the human brain. Hum. Brain Mapp. 41 (5), 1167–1180.
Mishra, A., Majumdar, S., Wang, F., Wilson, G.H., Gore 3rd, J.C., Chen, L.M., 2019. Functional connectivity with cortical depth assessed by resting state fMRI of subregions of S1 in squirrel monkeys. Hum. Brain Mapp. 40 (1), 329–339.
Mishra, A., Reynolds, J.P., Chen, Y., Gourine, A.V., Rusakov, D.A., Attwell, D., 2016. Astrocytes mediate neurovascular signaling to capillary pericytes but not to arterioles. Nat. Neurosci. 19 (12), 1619–1627.
Mishra, A.M., Ellens, D.J., Schridde, U., Motelow, J.E., Purcaro, M.J., DeSalvo, M.N., Enev, M., Sanganahalli, B.G., Hyder, F., Blumenfeld, H., 2011. Where fMRI and electrophysiology agree to disagree: corticothalamic and striatal activity patterns in the WAG/Rij rat. J. Neurosci. 31 (42), 15053–15064.
Mitra, A., Snyder, A.Z., Blazey, T., Raichle, M.E., 2015. Lag threads organize the brain's intrinsic activity. Proc. Natl. Acad. Sci. U. S. A. 112 (17), E2235–E2244.
Mitra, P.P., 2014. The circuit architecture of whole brains at the mesoscopic scale. Neuron 83 (6), 1273–1283.
Mitra, P.P., Ogawa, S., Hu, X., Ugurbil, K., 1997. The nature of spatiotemporal changes in cerebral hemodynamics as manifested in functional magnetic resonance imaging. Magn. Reson. Med. 37 (4), 511–518.
Mohajerani, M.H., Chan, A.W., Mohsenvand, M., LeDue, J., Liu, R., McVea, D.A., Boyd, J.D., Wang, Y.T., Reimers, M., Murphy, T.H., 2013. Spontaneous cortical activity alternates between motifs defined by regional axonal projections. Nat. Neurosci. 16 (10), 1426–1435.
Mohajerani, M.H., McVea, D.A., Fingas, M., Murphy, T.H., 2010. Mirrored bilateral slow-wave cortical activity within local circuits revealed by fast bihemispheric voltage-sensitive dye imaging in anesthetized and awake mice. J. Neurosci. 30 (10), 3745–3751.
Moon, H.S., Jiang, H., Vo, T.T., Jung, W.B., Vazquez, A.L., Kim, S.G., 2021. Contribution of Excitatory and Inhibitory Neuronal Activity to BOLD fMRI. Cereb. Cortex 31 (9), 4053–4067. doi:10.1093/cercor/bhab068.
Murphy, K., Birn, R.M., Bandettini, P.A., 2013. Resting-state fMRI confounds and cleanup. Neuroimage 80, 349–359.
Musch, K., Honey, C.J., 2018. Causal evidence for a neural component of spatially global hemodynamic signals. Neuron 97 (4), 734–736.
Nair, J., Klaassen, A.L., Arato, J., Vyssotski, A.L., Harvey, M., Rainer, G., 2018. Basal forebrain contributes to default mode network regulation. Proc. Natl. Acad. Sci. U. S. A. 115 (6), 1352–1357.
Nakai, J., Ohkura, M., Imoto, K., 2001. A high signal-to-noise Ca(2+) probe composed of a single green fluorescent protein. Nat. Biotechnol. 19 (2), 137–141.
Nelson, A.R., Sagare, M.A., Wang, Y., Kisler, K., Zhao, Z., Zlokovic, B.V., 2020. Channelrhodopsin Excitation Contracts Brain Pericytes and Reduces Blood Flow in the Aging Mouse Brain in vivo. Front. Aging Neurosci. 12, 108.
Neske, G.T., 2015. The slow oscillation in cortical and thalamic networks: mechanisms and functions. Front. Neural Circuits 9, 88.
Niell, C.M., Stryker, M.P., 2010. Modulation of visual responses by behavioral state in mouse visual cortex. Neuron 65 (4), 472–479.
Niessing, J., Ebisch, B., Schmidt, K.E., Niessing, M., Singer, W., Galuske, R.A., 2005. Hemodynamic signals correlate tightly with synchronized gamma oscillations. Science 309 (5736), 948–951.
Nir, Y., Mukamel, R., Dinstein, I., Privman, E., Harel, M., Fisch, L., Gelbard-Sagiv, H., Kipervasser, S., Andelman, F., Neufeld, M.Y., Kramer, U., Arieli, A., Fried, I., Malach, R., 2008. Interhemispheric correlations of slow spontaneous neuronal fluctuations revealed in human sensory cortex. Nat. Neurosci. 11 (9), 1100–1108.
Nishimura, N., Schaffer, C.B., Friedman, B., Lyden, P.D., Kleinfeld, D., 2007. Penetrating arterioles are a bottleneck in the perfusion of neocortex. Proc. Natl. Acad. Sci. U. S. A. 104 (1), 365–370.
Nizar, K., Uhlirova, H., Tian, P., Saisan, P.A., Cheng, Q., Reznichenko, L., Weldy, K.L., Steed, T.C., Sridhar, V.B., MacDonald, C.L., Cui, J., Gratiy, S.L., Sakadzic, S., Boas, D.A., Beka, T.I., Einevoll, G.T., Chen, J., Masliah, E., Dale, A.M., Silva, G.A., Devor, A., 2013. In vivo stimulus-induced vasodilation occurs without IP3 receptor activation and may precede astrocytic calcium increase. J. Neurosci. 33 (19), 8411–8422.
Ogawa, S., Lee, T.M., Nayak, A.S., Glynn, P., 1990. Oxygenation-sensitive contrast in magnetic resonance image of rodent brain at high magnetic fields. Magn. Reson. Med. 14 (1), 68–78.
Oh, J., Lee, C., Kaang, B.K., 2019. Imaging and analysis of genetically encoded calcium indicators linking neural circuits and behaviors. Korean J. Physiol. Pharmacol. 23 (4), 237–249.
Oh, S.W., Harris, J.A., Ng, L., Winslow, B., Cain, N., Mihalas, S., Wang, Q., Lau, C., Kuan, L., Henry, A.M., Mortrud, M.T., Ouellette, B., Nguyen, T.N., Sorensen, S.A., Slaughterbeck, C.R., Wakeman, W., Li, Y., Feng, D., Ho, A., Nicholas, E., Hirokawa, K.E., Bohn, P., Joines, K.M., Peng, H., Hawrylycz, M.J., Phillips, J.W., Hohmann, J.G., Wohnoutka, P., Gerfen, C.R., Koch, C., Bernard, A., Dang, C., Jones, A.R., Zeng, H., 2014. A mesoscale connectome of the mouse brain. Nature 508 (7495), 207–214.
Osmanski, B.F., Pezet, S., Ricobaraza, A., Lenkei, Z., Tanter, M., 2014. Functional ultrasound imaging of intrinsic connectivity in the living rat brain with high spatiotemporal resolution. Nat. Commun. 5, 5023.
Osol, G., Halpern, W., 1988. Spontaneous vasomotion in pressurized cerebral arteries from genetically hypertensive rats. Am. J. Physiol. 254 (1 Pt 2), H28–H33.
Otsu, Y., Couchman, K., Lyons, D.G., Collot, M., Agarwal, A., Mallet, J.M., Pfrieger, F.W., Bergles, D.E., Charpak, S., 2015. Calcium dynamics in astrocyte processes during neurovascular coupling. Nat. Neurosci. 18 (2), 210–218.
Ozbay, P.S., Chang, C., Picchioni, D., Mandelkow, H., Chappel-Farley, M.G., van Gelderen, P., de Zwart, J.A., Duyn, J., 2019. Sympathetic activity contributes to the fMRI signal. Commun. Biol. 2, 421.
Ozbay, P.S., Chang, C., Picchioni, D., Mandelkow, H., Moehlman, T.M., Chappel-Farley, M.G., van Gelderen, P., de Zwart, J.A., Duyn, J.H., 2018. Contribution of systemic vascular effects to fMRI activity in white matter. Neuroimage 176, 541–549.
Paasonen, J., Laakso, H., Pirttimaki, T., Stenroos, P., Salo, R.A., Zhurakovskaya, E., Lehto, L.J., Tanila, H., Garwood, M., Michaeli, S., Idiyatullin, D., Mangia, S., Grohn, O., 2020. Multi-band SWIFT enables quiet and artefact-free EEG-fMRI and awake fMRI studies in rat. Neuroimage 206, 116338.
Pais-Roldan, P., Biswal, B., Scheffler, K., Yu, X., 2018. Identifying respiration-related aliasing artifacts in the rodent resting-state fMRI. Front. Neurosci. 12, 788.
Pais-Roldan, P., Edlow, B.L., Jiang, Y., Stelzer, J., Zou, M., Yu, X., 2019. Multimodal assessment of recovery from coma in a rat model of diffuse brainstem tegmentum injury. Neuroimage 189, 615–630.
Pais-Roldan, P., Takahashi, K., Sobczak, F., Chen, Y., Zhao, X., Zeng, H., Jiang, Y., Yu, X., 2020. Indexing brain state-dependent pupil dynamics with simultaneous fMRI and optical fiber calcium recording. Proc. Natl. Acad. Sci. U. S. A. 117 (12), 6875–6882.
Pal, A., Tian, L., 2020. Imaging voltage and brain chemistry with genetically encoded sensors and modulators. Curr. Opin. Chem. Biol. 57, 166–176.
Palmer, A.E., Qin, Y., Park, J.G., McCombs, J.E., 2011. Design and application of genetically encoded biosensors. Trends Biotechnol. 29 (3), 144–152.
Palomero-Gallagher, N., Zilles, K., 2019. Cortical layers: cyto-, myelo-, receptor- and synaptic architecture in human cortical areas. Neuroimage 197, 716–741.
Pan, W.J., Lee, S.Y., Billings, J., Nezafati, M., Majeed, W., Buckley, E., Keilholz, S., 2018. Detection of neural light-scattering activity in vivo: optical transmittance studies in the rat brain. Neuroimage 179, 207–214.
Pan, W.J., Thompson, G., Magnuson, M., Majeed, W., Jaeger, D., Keilholz, S., 2011. Broadband local field potentials correlate with spontaneous fluctuations in functional magnetic resonance imaging signals in the rat somatosensory cortex under isoflurane anesthesia. Brain Connect. 1 (2), 119–131.
Pan, W.J., Thompson, G.J., Magnuson, M.E., Jaeger, D., Keilholz, S., 2013. Infraslow LFP correlates to resting-state fMRI BOLD signals. Neuroimage 74, 288–297.
Pearl, J., 2009. Causal inference in statistics: an overview. Stat. Surv. 3, 96–146.
Peeters, L.M., Hinz, R., Detrez, J.R., Missault, S., De Vos, W.H., Verhoye, M., Van der Linden, A., Keliris, G.A., 2020. Chemogenetic silencing of neurons in the mouse anterior cingulate area modulates neuronal activity and functional connectivity. Neuroimage 220, 117088.
Peeters, R.R., Tindemans, I., De Schutter, E., Van der Linden, A., 2001. Comparing BOLD fMRI signal changes in the awake and anesthetized rat during electrical forepaw stimulation. Magn. Reson. Imaging 19 (6), 821–826.
Perrenoud, Q., Geoffroy, H., Gauthier, B., Rancillac, A., Alfonsi, F., Kessaris, N., Rossier, J., Vitalis, T., Gallopin, T., 2012. Characterization of Type I and Type II nNOS-Expressing Interneurons in the Barrel Cortex of Mouse. Front. Neural Circuits 6, 36.
Perrenoud, Q., Rossier, J., Ferezou, I., Geoffroy, H., Gallopin, T., Vitalis, T., Rancillac, A., 2012. Activation of cortical 5-HT(3) receptor-expressing interneurons induces NO mediated vasodilatations and NPY mediated vasoconstrictions. Front. Neural Circuits 6, 50.
Petilla Interneuron Nomenclature, G., Ascoli, G.A., Alonso-Nanclares, L., Anderson, S.A., Barrionuevo, G., Benavides-Piccione, R., Burkhalter, A., Buzsaki, G., Cauli, B., Defelipe, J., Fairen, A., Feldmeyer, D., Fishell, G., Fregnac, Y., Freund, T.F., Gardner, D., Gardner, E.P., Goldberg, J.H., Helmstaedter, M., Hestrin, S., Karube, F., Kisvarday, Z.F., Lambolez, B., Lewis, D.A., Marin, O., Markram, H., Munoz, A., Packer, A., Petersen, C.C., Rockland, K.S., Rossier, J., Rudy, B., Somogyi, P., Staiger, J.F., Tamas, G., Thomson, A.M., Toledo-Rodriguez, M., Wang, Y., West, D.C., Yuste, R., 2008. Petilla terminology: nomenclature of features of GABAergic interneurons of the cerebral cortex. Nat. Rev. Neurosci. 9 (7), 557–568.
Petridou, N., Gaudes, C.C., Dryden, I.L., Francis, S.T., Gowland, P.A., 2013. Periods of rest in fMRI contain individual spontaneous events which are related to slowly fluctuating spontaneous activity. Hum. Brain Mapp. 34 (6), 1319–1329.
Pisanello, M., Pisano, F., Hyun, M., Maglie, E., Balena, A., De Vittorio, M., Sabatini, B.L., Pisanello, F., 2019. The Three-Dimensional Signal Collection Field for Fiber Photometry in Brain Tissue. Front. Neurosci. 13, 82.
Poplawsky, A.J., Fukuda, M., Murphy, M., Kim, S.G., 2015. Layer-Specific fMRI Responses to Excitatory and Inhibitory Neuronal Activities in the Olfactory Bulb. J. Neurosci. 35 (46), 15263–15275.
Power, J.D., Laumann, T.O., Plitt, M., Martin, A., Petersen, S.E., 2017a. On Global fMRI Signals and Simulations. Trends Cogn. Sci. 21 (12), 911–913.

Power, J.D., Plitt, M., Laumann, T.O., Martin, A., 2017b. Sources and implications of whole-brain fMRI signals in humans. Neuroimage 146, 609–625.
Raj, D., Paley, D.P., Anderson, A.W., Kennan, R.P., Gore, J.C., 2000. A model for susceptibility artefacts from respiration in functional echo-planar magnetic resonance imaging. Phys. Med. Biol. 45 (12), 3809–3820.
Rajkumar, R., Régio Brambilla, C., Veselinović, T., Bierbrier, J., Wyss, C., Ramkiran, S., Orth, L., Lang, M., Rota Kops, E., Mauler, J., Scheins, J., Neumaier, B., Ermert, J., Herzog, H., Langen, K-J., Binkofski, F-C, Lerche, C., Shah, NJ., Neuner, I., 2021. Excitatory–inhibitory balance within EEG microstates and resting-state fMRI networks: assessed via simultaneous trimodal PET–MR–EEG imaging. Transl. Psychiatry 11, 60.
Rasmussen, R., Nicholas, E., Petersen, N.C., Dietz, A.G., Xu, Q., Sun, Q., Nedergaard, M., 2019. Cortex-wide Changes in Extracellular Potassium Ions Parallel Brain State Transitions in Awake Behaving Mice. Cell Rep. 28 (5), 1182–1194 e1184.
Razoux, F., Baltes, C., Mueggler, T., Seuwen, A., Russig, H., Mansuy, I., Rudin, M., 2013. Functional MRI to assess alterations of functional networks in response to pharmacological or genetic manipulations of the serotonergic system in mice. Neuroimage 74, 326–336.
Reed, M.D., Pira, A.S., Febo, M., 2013. Behavioral effects of acclimatization to restraint protocol used for awake animal imaging. J. Neurosci. Methods 217 (1-2), 63–66.
Reveley, C., Seth, A.K., Pierpaoli, C., Silva, A.C., Yu, D., Saunders, R.C., Leopold, D.A., Ye, F.Q., 2015. Superficial white matter fiber systems impede detection of long-range cortical connections in diffusion MR tractography. Proc. Natl. Acad. Sci. U. S. A. 112 (21), E2820–E2828.
Rockstroh, B., Muller, M., Wagner, M., Cohen, R., Elbert, T., 1993. Probing" the nature of the CNV. Electroencephalogr. Clin. Neurophysiol. 87 (4), 235–241.
Roe, A.W., 2019. Columnar connectome: toward a mathematics of brain function. Netw. Neurosci. 3 (3), 779–791.
Rosenberg, M.D., Scheinost, D., Greene, A.S., Avery, E.W., Kwon, Y.H., Finn, E.S., Ramani, R., Qiu, M., Constable, R.T., Chun, M.M., 2020. Functional connectivity predicts changes in attention observed across minutes, days, and months. Proc. Natl. Acad. Sci. U. S. A. 117 (7), 3797–3807.
Rosler, F., Heil, M., Roder, B., 1997. Slow negative brain potentials as reflections of specific modular resources of cognition. Biol. Psychol. 45 (1-3), 109–141.
Rungta, R.L., Chaigneau, E., Osmanski, B.F., Charpak, S., 2018. Vascular Compartmentalization of Functional Hyperemia from the Synapse to the Pia. Neuron 99 (2), 362–375 e364.
Ryali, S., Shih, Y.Y., Chen, T., Kochalka, J., Albaugh, D., Fang, Z., Supekar, K., Lee, J.H., Menon, V., 2016. Combining optogenetic stimulation and fMRI to validate a multivariate dynamical systems model for estimating causal brain interactions. Neuroimage 132, 398–405.
Sabatini, B.L., Tian, L., 2020. Imaging Neurotransmitter and Neuromodulator Dynamics In Vivo with Genetically Encoded Indicators. Neuron 108 (1), 17–32.
Sakata, S., Harris, K.D., 2009. Laminar structure of spontaneous and sensory-evoked population activity in auditory cortex. Neuron 64 (3), 404–418.
Salimi-Khorshidi, G., Douaud, G., Beckmann, C.F., Glasser, M.F., Griffanti, L., Smith, S.M., 2014. Automatic denoising of functional MRI data: combining independent component analysis and hierarchical fusion of classifiers. Neuroimage 90, 449–468.
Sarter, M., Lustig, C., 2020. Forebrain cholinergic signaling: wired and phasic, not tonic, and causing behavior. J. Neurosci. 40 (4), 712–719.
Scheeringa, R., Koopmans, P.J., van Mourik, T., Jensen, O., Norris, D.G., 2016. The relationship between oscillatory EEG activity and the laminar-specific BOLD signal. Proc. Natl. Acad. Sci. U. S. A. 113 (24), 6761–6766.
Schilling, K., Gao, Y., Janve, V., Stepniewska, I., Landman, B.A., Anderson, A.W., 2018. Confirmation of a gyral bias in diffusion MRI fiber tractography. Hum. Brain Mapp. 39 (3), 1449–1466.
Schmidt, M., Bakker, R., Hilgetag, C.C., Diesmann, M., van Albada, S.J., 2018. Multi-scale account of the network structure of macaque visual cortex. Brain Struct. Funct. 223 (3), 1409–1435.
Scholvinck, M.L., Maier, A., Ye, F.Q., Duyn, J.H., Leopold, D.A., 2010. Neural basis of global resting-state fMRI activity. Proc. Natl. Acad. Sci. U. S. A. 107 (22), 10238–10243.
Schridde, U., Khubchandani, M., Motelow, J.E., Sanganahalli, B.G., Hyder, F., Blumenfeld, H., 2008. Negative BOLD with large increases in neuronal activity. Cereb. Cortex 18 (8), 1814–1827.
Schroeder, M.P., Weiss, C., Procissi, D., Disterhoft, J.F., Wang, L., 2016. Intrinsic connectivity of neural networks in the awake rabbit. Neuroimage 129, 260–267.
Schulz, K., Sydekum, E., Krueppel, R., Engelbrecht, C.J., Schlegel, F., Schroter, A., Rudin, M., Helmchen, F., 2012. Simultaneous BOLD fMRI and fiber-optic calcium recording in rat neocortex. Nat. Methods 9 (6), 597–602.
Sclocco, R., Beissner, F., Bianciardi, M., Polimeni, J.R., Napadow, V., 2018. Challenges and opportunities for brainstem neuroimaging with ultrahigh field MRI. Neuroimage 168, 412–426.
Scott, N.A., Murphy, T.H., 2012. Hemodynamic responses evoked by neuronal stimulation via channelrhodopsin-2 can be independent of intracortical glutamatergic synaptic transmission. PLoS One 7 (1), e29859.
Shah, D., Blockx, I., Guns, P.J., De Deyn, P.P., Van Dam, D., Jonckers, E., Delgado, Y.P.R., Verhoye, M., Van der Linden, A., 2015. Acute modulation of the cholinergic system in the mouse brain detected by pharmacological resting-state functional MRI. Neuroimage 109, 151–159.
Shah, D., Blockx, I., Keliris, G.A., Kara, F., Jonckers, E., Verhoye, M., Van der Linden, A., 2016. Cholinergic and serotonergic modulations differentially affect large-scale functional networks in the mouse brain. Brain Struct. Funct. 221 (6), 3067–3079.
Shakil, S., Lee, C.H., Keilholz, S.D., 2016. Evaluation of sliding window correlation performance for characterizing dynamic functional connectivity and brain states. Neuroimage 133, 111–128.
Sharoh, D., van Mourik, T., Bains, L.J., Segaert, K., Weber, K., Hagoort, P., Norris, D.G., 2019. Laminar specific fMRI reveals directed interactions in distributed networks during language processing. Proc. Natl. Acad. Sci. U. S. A. 116 (42), 21185–21190.
Sherman, S.M., Guillery, R.W., 2011. Distinct functions for direct and transthalamic corticocortical connections. J. Neurophysiol. 106 (3), 1068–1077.
Shi, Z., Wu, R., Yang, P.F., Wang, F., Wu, T.L., Mishra, A., Chen, L.M., Gore, J.C., 2017. High spatial correspondence at a columnar level between activation and resting state fMRI signals and local field potentials. Proc. Natl. Acad. Sci. U. S. A. 114 (20), 5253–5258.
Shih, Y.Y., Chen, Y.Y., Lai, H.Y., Kao, Y.C., Shyu, B.C., Duong, T.Q., 2013. Ultra high-resolution fMRI and electrophysiology of the rat primary somatosensory cortex. Neuroimage 73, 113–120.
Shih, Y-Y., Chen, C-C., Shyu, B-C., Lin, Z-J., Chiang, Y-C., Jaw, F.-S., Chen, Y-Y., Chen, C., 2009. A new scenario for negative functional magnetic resonance imaging signals: endogenous neurotransmission. J Neurosci 29 (10), 3036–3044 PMID: 19279240.
Shih, Y.-Y., Wey, H-Y., de la Garza, B.H., Duong, T.Q., 2011. Striatal and cortical BOLD, blood flow, blood volume, oxygen consumption, and glucose consumption changes in noxious forepaw electrical stimulation. J Cereb Blood Flow Metab 31 (3), 832–841 PMID: 20940730.
Shih, Y-Y., Huang, S., Chen, Y.-Y., Lai, H-Y., Kao, Y-C., Du, F., Hue, E.S., Duong, T.Q, 2014. Imaging neurovascular function and functional recovery after stroke in the rat striatum using forepaw stimulation. J Cereb Blood Flow Metab 34 (9), 1483–1492 PMID: 24917039.
Shmuel, A., Leopold, D.A., 2008. Neuronal correlates of spontaneous fluctuations in fMRI signals in monkey visual cortex: Implications for functional connectivity at rest. Hum. Brain Mapp. 29 (7), 751–761.
Shokri-Kojori, E., Tomasi, D., Volkow, N.D., 2018. An Autonomic Network: Synchrony Between Slow Rhythms of Pulse and Brain Resting State Is Associated with Personality and Emotions. Cereb. Cortex 28 (9), 3356–3371.
Siero, J.C., Hendrikse, J., Hoogduin, H., Petridou, N., Luijten, P., Donahue, M.J., 2015. Cortical depth dependence of the BOLD initial dip and poststimulus undershoot in human visual cortex at 7 Tesla. Magn. Reson. Med. 73 (6), 2283–2295.
Silva, A.C., Koretsky, A.P., 2002. Laminar specificity of functional MRI onset times during somatosensory stimulation in rat. Proc. Natl. Acad. Sci. U. S. A. 99 (23), 15182–15187.
Silva, A.C., Lee, S.P., Yang, G., Iadecola, C., Kim, S.G., 1999. Simultaneous blood oxygenation level-dependent and cerebral blood flow functional magnetic resonance imaging during forepaw stimulation in the rat. J. Cereb. Blood Flow Metab. 19 (8), 871–879.
Smith, S.M., Fox, P.T., Miller, K.L., Glahn, D.C., Fox, P.M., Mackay, C.E., Filippini, N., Watkins, K.E., Toro, R., Laird, A.R., Beckmann, C.F., 2009. Correspondence of the brain's functional architecture during activation and rest. Proc. Natl. Acad. Sci. U. S. A. 106 (31), 13040–13045.
Stenroos, P., Paasonen, J., Salo, R.A., Jokivarsi, K., Shatillo, A., Tanila, H., Grohn, O., 2018. Awake Rat Brain Functional Magnetic Resonance Imaging Using Standard Radio Frequency Coils and a 3D Printed Restraint Kit. Front. Neurosci. 12, 548.
Stringer, C., Pachitariu, M., Steinmetz, N., Reddy, C.B., Carandini, M., Harris, K.D., 2019. Spontaneous behaviors drive multidimensional, brainwide activity. Science 364 (6437), 255.
Sych, Y., Chernysheva, M., Sumanovski, L.T., Helmchen, F., 2019. High-density multi-fiber photometry for studying large-scale brain circuit dynamics. Nat. Methods 16 (6), 553–560.
Tagliazucchi, E., Balenzuela, P., Fraiman, D., Chialvo, D.R., 2012. Criticality in large-scale brain FMRI dynamics unveiled by a novel point process analysis. Front. Physiol. 3, 15.
Tagliazucchi, E., Laufs, H., 2014. Decoding wakefulness levels from typical fMRI resting-state data reveals reliable drifts between wakefulness and sleep. Neuron 82 (3), 695–708.
Takata, N., Sugiura, Y., Yoshida, K., Koizumi, M., Hiroshi, N., Honda, K., Yano, R., Komaki, Y., Matsui, K., Suematsu, M., Mimura, M., Okano, H., Tanaka, K.F., 2018. Optogenetic astrocyte activation evokes BOLD fMRI response with oxygen consumption without neuronal activity modulation. Glia 66 (9), 2013–2023.
Teichert, T., Grinband, J., Hirsch, J., Ferrera, V.P., 2010. Effects of heartbeat and respiration on macaque fMRI: implications for functional connectivity. Neuropsychologia 48 (7), 1886–1894.
Thompson, G.J., Merritt, M.D., Pan, W.J., Magnuson, M.E., Grooms, J.K., Jaeger, D., Keilholz, S.D., 2013. Neural correlates of time-varying functional connectivity in the rat. Neuroimage 83, 826–836.
Thompson, G.J., Pan, W.J., Magnuson, M.E., Jaeger, D., Keilholz, S.D., 2014. Quasi-periodic patterns (QPP): large-scale dynamics in resting state fMRI that correlate with local infraslow electrical activity. Neuroimage 84, 1018–1031.
Tian, L., Hires, S.A., Mao, T., Huber, D., Chiappe, M.E., Chalasani, S.H., Petreanu, L., Akerboom, J., McKinney, S.A., Schreiter, E.R., Bargmann, C.I., Jayaraman, V., Svoboda, K., Looger, L.L., 2009. Imaging neural activity in worms, flies and mice with improved GCaMP calcium indicators. Nat. Methods 6 (12), 875–881.
Tong, L., Hill, R.A., Damisah, E.C., Murray, K.N., Yuan, P., Bordey, A., Grutzendler, J., 2021. Imaging and optogenetic modulation of vascular mural cells in the live brain. Nat. Protoc. 16 (1), 472–496.
Tong, Y., Hocke, L.M., Nickerson, L.D., Licata, S.C., Lindsey, K.P., Frederick, B., 2013. Evaluating the effects of systemic low frequency oscillations measured in the periphery on the independent component analysis results of resting state networks. Neuroimage 76, 202–215.
Torres-Gomez, S., Blonde, J.D., Mendoza-Halliday, D., Kuebler, E., Everest, M., Wang, X.J., Inoue, W., Poulter, M.O., Martinez-Trujillo, J., 2020. Changes in the proportion of inhibitory interneuron types from sensory to executive areas of the primate neocortex: implications for the origins of working memory representations. Cereb. Cortex 30 (8), 4544–4562.
Totah, N.K., Neves, R.M., Panzeri, S., Logothetis, N.K., Eschenko, O., 2018. The locus coeruleus is a complex and differentiated neuromodulatory system. Neuron 99 (5), 1055–1068 e1056.

Tran, C.H.T., Peringod, G., Gordon, G.R., 2018. Astrocytes integrate behavioral state and vascular signals during functional hyperemia. Neuron 100 (5), 1133–1148 e1133.
Tremblay, R., Lee, S., Rudy, B., 2016. GABAergic interneurons in the neocortex: from cellular properties to circuits. Neuron 91 (2), 260–292.
Tsai, P.S., Mateo, C., Field, J.J., Schaffer, C.B., Anderson, M.E., Kleinfeld, D., 2015. Ultra--large field-of-view two-photon microscopy. Opt. Express 23 (11), 13833–13847.
Turchi, J., Chang, C., Ye, F.Q., Russ, B.E., Yu, D.K., Cortes, C.R., Monosov, I.E., Duyn, J.H., Leopold, D.A., 2018. The basal forebrain regulates global resting-state fMRI fluctuations. Neuron 97 (4), 940–952 e944.
Turner, R., 2002. How much cortex can a vein drain? Downstream dilution of activation-related cerebral blood oxygenation changes. Neuroimage 16 (4), 1062–1067.
Uhlirova, H., Kilic, K., Tian, P., Thunemann, M., Desjardins, M., Saisan, P.A., Sakadzic, S., Ness, T.V., Mateo, C., Cheng, Q., Weldy, K.L., Razoux, F., Vandenberghe, M., Cremonesi, J.A., Ferri, C.G., Nizar, K., Sridhar, V.B., Steed, T.C., Abashin, M., Fainman, Y., Masliah, E., Djurovic, S., Andreassen, O.A., Silva, G.A., Boas, D.A., Kleinfeld, D., Buxton, R.B., Einevoll, G.T., Dale, A.M., Devor, A., 2016. Cell type specificity of neurovascular coupling in cerebral cortex. Elife 5, e14315. doi:10.7554/eLife.14315, PMID: 27244241.
Uludag, K., Blinder, P., 2018. Linking brain vascular physiology to hemodynamic response in ultra-high field MRI. Neuroimage 168, 279–295.
Urban-Ciecko, J., Barth, A.L., 2016. Somatostatin-expressing neurons in cortical networks. Nat. Rev. Neurosci. 17 (7), 401–409.
Urban, A., Mace, E., Brunner, C., Heidmann, M., Rossier, J., Montaldo, G., 2014. Chronic assessment of cerebral hemodynamics during rat forepaw electrical stimulation using functional ultrasound imaging. Neuroimage 101, 138–149.
Urban, A., Rancillac, A., Martinez, L., Rossier, J., 2012. Deciphering the neuronal circuitry controlling local blood flow in the cerebral cortex with optogenetics in PV::cre transgenic mice. Front. Pharmacol. 3, 105.
Van den Berge, N., Albaugh, D.L., Salzwedel, A., Vanhove, C., Van Holen, R., Gao, W., Stuber, G.D., Shih, Y-Y, 2017. Functional circuit mapping of striatal output nuclei using simultaneous deep brain stimulation and fMRI. Neuroimage 146, 1050–1061 PMID: 27825979.
van den Brink, R.L., Pfeffer, T., Donner, T.H., 2019. Brainstem modulation of large-scale intrinsic cortical activity correlations. Front. Hum. Neurosci. 13, 340.
van den Heuvel, M.P., Sporns, O., 2011. Rich-club organization of the human connectome. J. Neurosci. 31 (44), 15775–15786.
Van Essen, D.C., Smith, S.M., Barch, D.M., Behrens, T.E., Yacoub, E., Ugurbil, K., Consortium, W.U.M.H., 2013. The WU-minn human connectome project: an overview. Neuroimage 80, 62–79.
van Houdt, P.J., Ossenblok, P.P., Boon, P.A., Leijten, F.S., Velis, D.N., Stam, C.J., de Munck, J.C., 2010. Correction for pulse height variability reduces physiological noise in functional MRI when studying spontaneous brain activity. Hum. Brain Mapp. 31 (2), 311–325.
Vanhaudenhuyse, A., Noirhomme, Q., Tshibanda, L.J., Bruno, M.A., Boveroux, P., Schnakers, C., Soddu, A., Perlbarg, V., Ledoux, D., Brichant, J.F., Moonen, G., Maquet, P., Greicius, M.D., Laureys, S., Boly, M., 2010. Default network connectivity reflects the level of consciousness in non-communicative brain-damaged patients. Brain 133 (Pt 1), 161–171.
Vanni, M.P., Chan, A.W., Balbi, M., Silasi, G., Murphy, T.H., 2017. Mesoscale mapping of mouse cortex reveals frequency-dependent cycling between distinct macroscale functional modules. J. Neurosci. 37 (31), 7513–7533.
Vasireddi, A.K., Vazquez, A.L., Whitney, D.E., Fukuda, M., Kim, S.G., 2016. Functional connectivity of resting hemodynamic signals in submillimeter orientation columns of the visual cortex. Brain Connect. 6 (8), 596–606.
Vazquez-Rodriguez, B., Suarez, L.E., Markello, R.D., Shafiei, G., Paquola, C., Hagmann, P., van den Heuvel, M.P., Bernhardt, B.C., Spreng, R.N., Misic, B., 2019. Gradients of structure-function tethering across neocortex. Proc. Natl. Acad. Sci. U. S. A. 116 (42), 21219–21227.
Vazquez, A.L., Fukuda, M., Crowley, J.C., Kim, S.G., 2014. Neural and hemodynamic responses elicited by forelimb- and photo-stimulation in channelrhodopsin-2 mice: insights into the hemodynamic point spread function. Cereb. Cortex 24 (11), 2908–2919.
Vazquez, A.L., Fukuda, M., Kim, S.G., 2018. Inhibitory neuron activity contributions to hemodynamic responses and metabolic load examined using an inhibitory optogenetic mouse model. Cereb. Cortex 28 (11), 4105–4119.
Vidaurre, D., Smith, S.M., Woolrich, M.W., 2017. Brain network dynamics are hierarchically organized in time. Proc. Natl. Acad. Sci. U. S. A. 114 (48), 12827–12832.
Vincent, J.L., Patel, G.H., Fox, M.D., Snyder, A.Z., Baker, J.T., Van Essen, D.C., Zempel, J.M., Snyder, L.H., Corbetta, M., Raichle, M.E., 2007. Intrinsic functional architecture in the anaesthetized monkey brain. Nature 447 (7140), 83–86.
Voipio, J., Tallgren, P., Heinonen, E., Vanhatalo, S., Kaila, K., 2003. Millivolt-scale DC shifts in the human scalp EEG: evidence for a nonneuronal generator. J. Neurophysiol. 89 (4), 2208–2214.
Wang, M., He, Y., Sejnowski, T.J., Yu, X., 2018. Brain-state dependent astrocytic Ca(2+) signals are coupled to both positive and negative BOLD-fMRI signals. Proc. Natl. Acad. Sci. U. S. A. 115 (7), E1647–E1656.
Wang, X., Leong, A.T.L., Chan, R.W., Liu, Y., Wu, E.X., 2019. Thalamic low frequency activity facilitates resting-state cortical interhemispheric MRI functional connectivity. Neuroimage 201, 115985.
Watakabe, A., Hirokawa, J., 2018. Cortical networks of the mouse brain elaborate within the gray matter. Brain Struct. Funct. 223 (8), 3633–3652.
Weber, B., Keller, A.L., Reichold, J., Logothetis, N.K., 2008. The microvascular system of the striate and extrastriate visual cortex of the macaque. Cereb. Cortex 18 (10), 2318–2330.
Weiler, N., Wood, L., Yu, J., Solla, S.A., Shepherd, G.M., 2008. Top-down laminar organization of the excitatory network in motor cortex. Nat Neurosci 11 (3), 360–366.
Whitesell, J.D., Liska, A., Coletta, L., Hirokawa, K.E., Bohn, P., Williford, A., Groblewski, P.A., Graddis, N., Kuan, L., Knox, J.E., Ho, A., Wakeman, W., Nicovich, P.R., Nguyen, T.N., van Velthoven, C.T.J., Garren, E., Fong, O., Naeemi, M., Henry, A.M., Dee, N., Smith, K.A., Levi, B., Feng, D., Ng, L., Tasic, B., Zeng, H., Mihalas, S., Gozzi, A., Harris, J.A., 2021. Regional, layer, and cell-type-specific connectivity of the mouse default mode network. Neuron 109 (3), 545–559 e548.
Williams, K.A., Magnuson, M., Majeed, W., LaConte, S.M., Peltier, S.J., Hu, X., Keilholz, S.D., 2010. Comparison of alpha-chloralose, medetomidine and isoflurane anesthesia for functional connectivity mapping in the rat. Magn. Reson. Imaging 28 (7), 995–1003.
Winder, A.T., Echagarruga, C., Zhang, Q., Drew, P.J., 2017. Weak correlations between hemodynamic signals and ongoing neural activity during the resting state. Nat. Neurosci. 20 (12), 1761–1769.
Wise, R.G., Ide, K., Poulin, M.J., Tracey, I., 2004. Resting fluctuations in arterial carbon dioxide induce significant low frequency variations in BOLD signal. Neuroimage 21 (4), 1652–1664.
Woodward, N.D., Cascio, C.J., 2015. Resting-state functional connectivity in psychiatric disorders. JAMA Psychiatry 72 (8), 743–744.
Wright, P.W., Brier, L.M., Bauer, A.Q., Baxter, G.A., Kraft, A.W., Reisman, M.D., Bice, A.R., Snyder, A.Z., Lee, J.M., Culver, J.P., 2017. Functional connectivity structure of cortical calcium dynamics in anesthetized and awake mice. PLoS One 12 (10), e0185759.
Wycoco, V., Shroff, M., Sudhakar, S., Lee, W., 2013. White matter anatomy: what the radiologist needs to know. Neuroimaging Clin. N. Am. 23 (2), 197–216.
Xu, A.G., Qian, M., Tian, F., Xu, B., Friedman, R.M., Wang, J., Song, X., Sun, Y., Chernov, M.M., Cayce, J.M., Jansen, E.D., Mahadevan-Jansen, A., Zhang, X., Chen, G., Roe, A.W., 2019. Focal infrared neural stimulation with high-field functional MRI: A rapid way to map mesoscale brain connectomes. Sci. Adv. 5 (4), eaau7046.
Yamashita, M., Yoshihara, Y., Hashimoto, R., Yahata, N., Ichikawa, N., Sakai, Y., Yamada, T., Matsukawa, N., Okada, G., Tanaka, S.C., Kasai, K., Kato, N., Okamoto, Y., Seymour, B., Takahashi, H., Kawato, M., Imamizu, H., 2018. A prediction model of working memory across health and psychiatric disease using whole-brain functional connectivity. Elife 7, e38844. doi:10.7554/eLife.38844, PMID: 30526859.
Yan, C.G., Chen, X., Li, L., Castellanos, F.X., Bai, T.J., Bo, Q.J., Cao, J., Chen, G.M., Chen, N.X., Chen, W., Cheng, C., Cheng, Y.Q., Cui, X.L., Duan, J., Fang, Y.R., Gong, Q.Y., Guo, W.B., Hou, Z.H., Hu, L., Kuang, L., Li, F., Li, K.M., Li, T., Liu, Y.S., Liu, Z.N., Long, Y.C., Luo, Q.H., Meng, H.Q., Peng, D.H., Qiu, H.T., Qiu, J., Shen, Y.D., Shi, Y.S., Wang, C.Y., Wang, F., Wang, K., Wang, L., Wang, X., Wang, Y., Wu, X.P., Wu, X.R., Xie, C.M., Xie, G.R., Xie, H.Y., Xie, P., Xu, X.F., Yang, H., Yang, J., Yao, J.S., Yao, S.Q., Yin, Y.Y., Yuan, Y.G., Zhang, A.X., Zhang, H., Zhang, K.R., Zhang, L., Zhang, Z.J., Zhou, R.B., Zhou, Y.T., Zhu, J.J., Zou, C.J., Si, T.M., Zuo, X.N., Zhao, J.P., Zang, Y.F., 2019. Reduced default mode network functional connectivity in patients with recurrent major depressive disorder. Proc. Natl. Acad. Sci. U. S. A. 116 (18), 9078–9083.
Yeh, C.H., Jones, D.K., Liang, X., Descoteaux, M., Connelly, A., 2020. Mapping structural connectivity using diffusion mri: challenges and opportunities. J. Magn. Reson. Imaging.
Yeo, B.T., Krienen, F.M., Sepulcre, J., Sabuncu, M.R., Lashkari, D., Hollinshead, M., Roffman, J.L., Smoller, J.W., Zollei, L., Polimeni, J.R., Fischl, B., Liu, H., Buckner, R.L., 2011. The organization of the human cerebral cortex estimated by intrinsic functional connectivity. J. Neurophysiol. 106 (3), 1125–1165.
Yoshikawa, A., Masaoka, Y., Yoshida, M., Koiwa, N., Honma, M., Watanabe, K., Kubota, S., Natsuko, I., Ida, M., Izumizaki, M., 2020. Heart rate and respiration affect the functional connectivity of default mode network in resting-state functional magnetic resonance imaging. Front. Neurosci. 14, 631.
Yousefi, B., Keilholz, S., 2021. Propagating patterns of intrinsic activity along macroscale gradients coordinate functional connections across the whole brain. Neuroimage, 117827.
Yousefi, B., Shin, J., Schumacher, E.H., Keilholz, S.D., 2018. Quasi-periodic patterns of intrinsic brain activity in individuals and their relationship to global signal. Neuroimage 167, 297–308.
Yu, X., He, Y., Wang, M., Merkle, H., Dodd, S.J., Silva, A.C., Koretsky, A.P., 2016. Sensory and optogenetically driven single-vessel fMRI. Nat. Methods 13 (4), 337–340.
Yu, X., Qian, C., Chen, D.Y., Dodd, S.J., Koretsky, A.P., 2014. Deciphering laminar-specific neural inputs with line-scanning fMRI. Nat. Methods 11 (1), 55–58.
Zaborszky, L., Gombkoto, P., Varsanyi, P., Gielow, M.R., Poe, G., Role, L.W., Ananth, M., Rajebhosale, P., Talmage, D.A., Hasselmo, M.E., Dannenberg, H., Minces, V.H., Chiba, A.A., 2018. Specific basal forebrain-cortical cholinergic circuits coordinate cognitive operations. J. Neurosci. 38 (44), 9446–9458.
Zerbi, V., Floriou-Servou, A., Markicevic, M., Vermeiren, Y., Sturman, O., Privitera, M., von Ziegler, L., Ferrari, K.D., Weber, B., De Deyn, P.P., Wenderoth, N., Bohacek, J., 2019. Rapid reconfiguration of the functional connectome after chemogenetic locus coeruleus activation. Neuron 103 (4), 702–718 e705.
Zerbi, V., Grandjean, J., Rudin, M., Wenderoth, N., 2015. Mapping the mouse brain with rs-fMRI: An optimized pipeline for functional network identification. Neuroimage 123, 11–21.
Zhang, X., Pan, W.J., Keilholz, S., 2019. The relationship between local field potentials and the blood-oxygenation-level dependent mri signal can be non-linear. Front. Neurosci. 13, 1126.
Zhang, X., Pan, W.J., Keilholz, S.D., 2020. The relationship between BOLD and neural activity arises from temporally sparse events. Neuroimage 207, 116390.